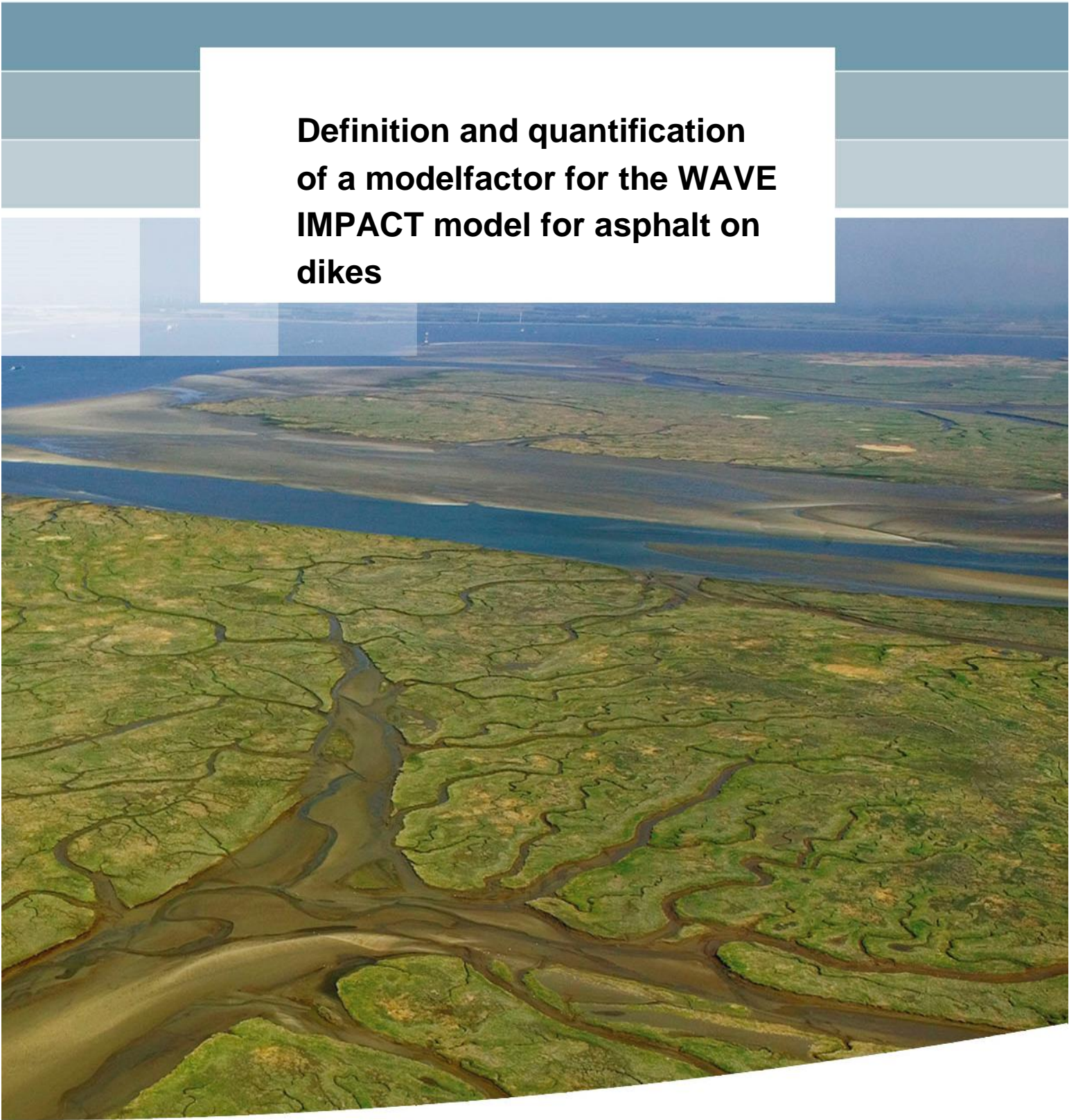


**Definition and quantification  
of a modelfactor for the WAVE  
IMPACT model for asphalt on  
dikes**





**Definition and quantification of a  
modelfactor for the WAVE IMPACT  
model for asphalt on dikes**

WTI-2017 product 5.15

dr. B.G.H.M. Wichman

1209437-021



**Title**

Definition and quantification of a model factor for the WAVE IMPACT model for asphalt on dikes

<b>Client</b> Rijkswaterstaat WVL	<b>Project</b> 1209437-021	<b>Reference</b> 1209437-021-HYE-0006- gbh	<b>Pages</b> 42
--------------------------------------	-------------------------------	--	--------------------



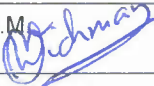
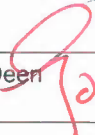

**Keywords**

Wave impact, modelling, asphalt, revetment, partial safety factors

**Summary**

In the project WTI-2017 a safety assessment for Dutch flood defences is being developed. Part of this project is cluster 5: safety assessment rules for revetments and grass covers on dikes. Part of this cluster is the development of assessment rules for asphaltic revetments on dikes. This report is referring to failure mechanism WAVE ATTACK (Golfklap). The current report is WTI-2017 product 5.15 and deals with the so called model factor.

A summary is given of all aspects that have to be taken into account for the determination of the amount of safety in the assessment with the WAVE IMPACT model. In order to quantify the uncertainty in this safety assessment, a model factor on the Miner's sum is introduced. In this report an analysis is given in order to obtain a probability distribution for this model factor. The wave impact assessment model is described as well as some considerations as to the input parameters. A discussion is given on the aspects influencing the safety, as well as an analysis to obtain the contribution of these aspects to the overall safety level (model factor). A value for the model factor  $\gamma_m$  is derived. Also a statistical distribution for the model uncertainty factor "m" has been derived by using estimates of the maximum en minimum of the contributing aspects.  $\gamma_m$  is the most probable safety factor value from this statistical distribution. This information has been used by WTI-2017 cluster C to calibrate the partial safety factor  $\gamma_s^*$  that is related to the target safety level and the uncertainty in WAVE IMPACT input parameters. Both safety factors will be used in a semi-probabilistic assessment rule. A method is proposed to estimate the outcome of the coming assessment for several representative cases, using the model factor  $\gamma_m$  and the partial safety factor  $\gamma_s^*$ , and on the basis of findings from previous assessments and experiences of water boards. More research is needed on how the observed spatial variations can be averaged in the zone where damage due to wave attack is expected. Also the analysis of the Falling Weight Deflectometer measurements has to be evaluated.

Version	Date	Author	Initials	Review	Initials	Approval	Initials
	Sept. 2014	dr. B.G.H.M. Wichman		ir. E. Calle		ir. L. Voogt	
	Dec. 2014	Dr. B.G.H.M. Wichman		Dr. J.K. van Deen		Ir. L. Voogt	

**State**  
final



## Content

<b>1</b>	<b>Introduction</b>	<b>1</b>
1.1	Context: deliverable to the WTI-2017 project	1
1.2	Aim of current report	4
1.3	Reader's guide	5
<b>2</b>	<b>Description of WAVE IMPACT assessment (WTI-2017)</b>	<b>7</b>
2.1	The WAVE IMPACT model	7
2.2	Failure in deterministic approach (previous safety assessment)	9
2.3	Input parameters	10
2.4	The WTI-2017 safety assessment steps	16
2.5	Modified failure criterion and safety factors	16
<b>3</b>	<b>Safety of WAVE IMPACT assessment</b>	<b>19</b>
3.1	Overview of aspects influencing safety	19
3.2	How to assess the amount of safety in the WAVE IMPACT model	19
3.3	Effect of limitations and inaccuracies of WAVE IMPACT model	21
3.3.1	Subsoil schematisation (aspect 1a)	21
3.3.2	Schematisation of wave impact (aspect 1b)	26
3.3.3	Determination of number of significant wave loadings (aspect 1c)	28
3.3.4	Assumption of uniform material parameters across the slope (aspect 1d)	29
3.4	Effect of uncertainty in the calculation of the Miner's sum (failure criterion, aspect 2)	29
3.5	Effect of irregularities in the structure (aspect 3)	29
3.6	Degree of saturation of dike body (aspect 4)	30
3.7	Assumptions and uncertainties in the determination of the WAVE IMPACT input parameters (aspect 5)	31
3.8	Effect of (high) temperature (aspect 6)	31
3.9	Residual strength as to the growth of cracks after initial failure (aspect 7)	32
<b>4</b>	<b>Assessment of probability distribution for the WAVE IMPACT model factor</b>	<b>33</b>
4.1	Overview of partial factors in the model factor $\gamma_m$	33
4.2	Choice of statistical distribution for "m" and a choice for model factor $\gamma_m$ .	34
4.3	Application for a set of representative cases: trial safety assessment	36
<b>5</b>	<b>Conclusions and recommendations</b>	<b>39</b>
5.1	Conclusions	39
5.2	Recommendations	39
<b>6</b>	<b>References</b>	<b>41</b>





# 1 Introduction

## 1.1 Context: deliverable to the WTI-2017 project

In the project WTI-2017 a safety assessment for Dutch flood defences is under development. Part of this project is cluster 5: safety assessment rules for revetments and grass covers on dikes. Part of this cluster is the development of assessment rules for asphaltic revetments on dikes. This report is referring to failure mechanism WAVE ATTACK (Golfklap), see failure mechanism 1, as given below. The current report is WTI-2017 product 5.15 and deals with the so called model factor, see section 1.2.

For asphaltic revetments on dikes in WTI-2017 a distinction has been made between three failure mechanisms:

1. Failure under wave attack (assessment by means of the WAVE IMPACT model, see figure 1.1).
2. Material transport through damages, as for example fissures (judgement of initial damage before the storm).
3. Uplift of the revetment due to a pressure head in the dike body.

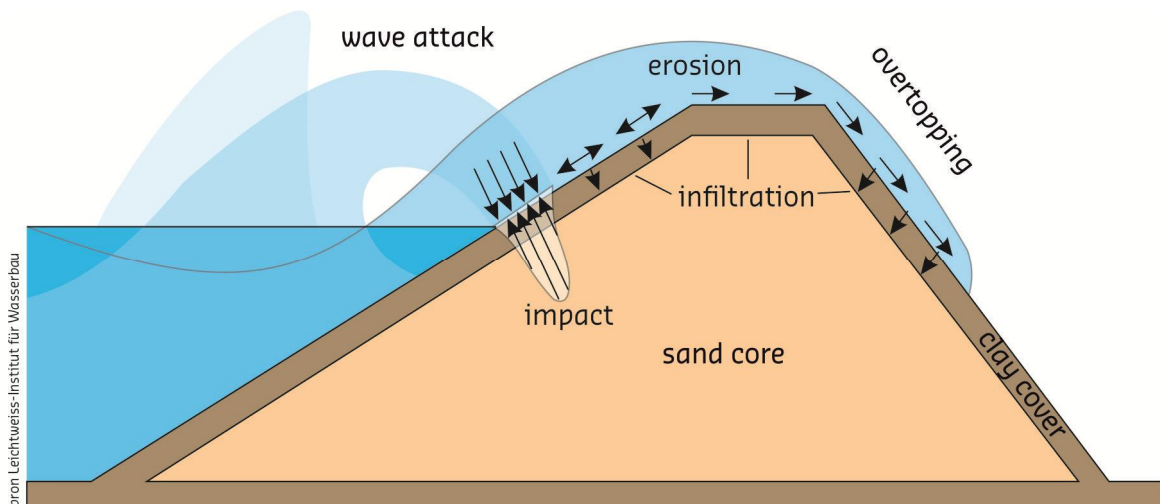


Figure 1.1 Failure mechanisms during wave attack on a dike (in the wave attack zone a protection is normally needed; in this case it is an asphalt layer)

The fault tree that will be a part of the WTI-2017 safety assessment is as follows, see Figure 1.2.

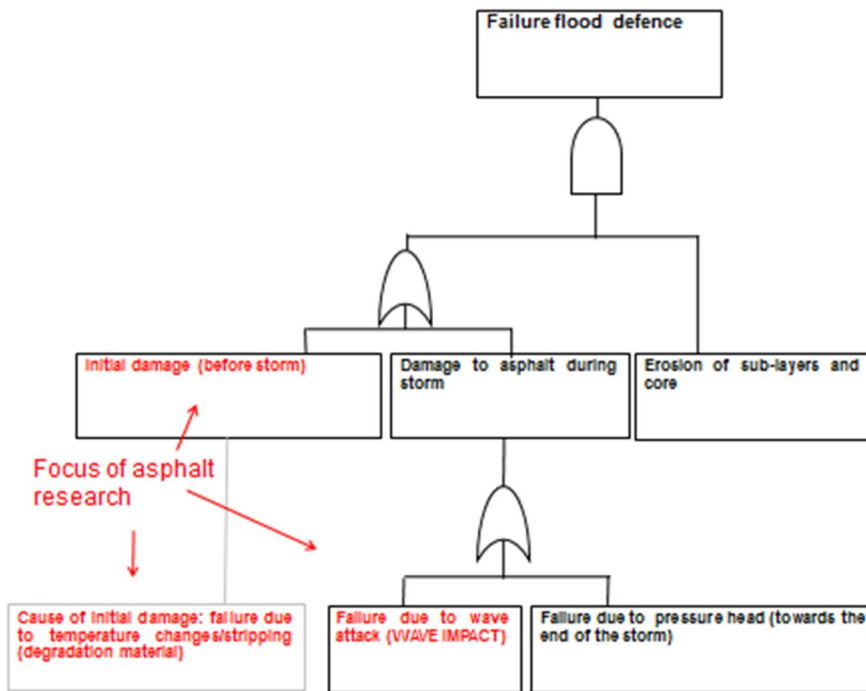


Figure 1.2 Fault tree for an asphaltic revetment. The topics of the current research are indicated in red.

The asphalt properties are changing due to temperature changes (in the worst leading to “temperature induced fissures”) and also due the effect of intrusion of moisture (stripping, see figure 1.3). The mechanical properties change due these processes and, therefore, the strength of the asphalt has to be assessed periodically. For failure mechanism 1 this is prescribed.

In addition, visual inspection and non-destructive monitoring is needed in order to detect damages.



Figure 1.3 Stripping problem at Harlingen Noorderpier.

For the assessment of the safety of the asphaltic revetment under wave attack, use is made of the model WAVE IMPACT (previously called "Golfklap"). The theoretical basis of this model is described in [1]. The functional design of the model WAVE IMPACT is described in [2]. The acquisition of input parameters is described in [3].

The WAVE IMPACT (Golfklap) model is normally in use for two types of asphaltic revetments: asphaltic concrete (hydraulic type, Waterbouw Asphalt Beton) and open stone asphalt (Open Steen Asphalt). 80% of the 600 km Dutch asphaltic revetments consist of hydraulic asphaltic concrete (WAB). About 10% is open stone asphalt (OSA), which is mainly applied on the dike slopes well above the wave attack zone. 80% of the asphalt is older than 30 years, which has as a consequence that a periodic safety assessment and maintenance actions are needed. For asphaltic concrete a significant amount of experience was gained during the last three periodic safety assessments, whereas for open stone asphalt the assessment method is not mature yet and in the past hardly any safety assessment was executed for open stone asphalt.

The aim of the current research on failure mechanism 1 is to validate the safety assessment method using the WAVE IMPACT model. This means that the safety of the model has to be validated, including the schematisation of the wave attack problem and the determination of its input parameters. The validation consists of experimental research, numerical calculations, sensitivity analyses, and a literature survey. In [4] the findings concerning this validation are described on the basis of experimental research (i.e. WTI-2017 product 5.14).

In the safety assessment as performed in the past use was made of the deterministic Golfklap model and characteristic values for its input parameters were taken. The WTI-2017 assessment is based on this approach. However, to obtain a fully probabilistic approach a model factor was introduced, see section 1.2. And for the semi-probabilistic assessment a

partial safety factor  $\gamma_s^*$  is needed to relate the semi-probabilistic safety format to the maximum allowable probability of failure.

## 1.2 Aim of current report

The aim of this report (WTI-2017 product 5.15) is to give a summary of all aspects that have to be taken into account for the assessment of the safety of the WAVE IMPACT model. This safety assessment says that the probability of failure should be lower than a specified local norm. In order to quantify the uncertainty in this safety assessment, a model factor on the Miner's sum is introduced. This is common practice when performing a probabilistic analysis. In this report an analysis is given in order to obtain a probability distribution for this model factor. A value for the model factor  $\gamma_m$  is derived, and also a statistical distribution for the model uncertainty factor "m" has been derived by using estimates of the maximum en minimum of the contributing aspects.  $\gamma_m$  is the most likely value for the model factor from the statistical distribution. This information will be used by WTI-2017 cluster C to calibrate the partial safety factor  $\gamma_s^*$  that is related to the target safety level and the uncertainty in WAVE IMPACT input parameters. Both safety factors will be used in a semi-probabilistic assessment rule.

In [5] (rapport veiligheid, in Dutch) a description is given of all aspects that play a role in the assessment of the safety of the asphaltic revetment under wave attack by means of the WAVE IMPACT model. In [5] it is also reviewed how the assessment was done in the past in a deterministic way, and what is needed to make a (semi-) probabilistic analysis in WTI-2017. Use will be made of the analysis of experimental results (see [4]) in order to quantify several aspects that have to be taken into account to derive the model factor.

In the current report a definition of the model factor is given. This factor accounts for uncertainties and inaccuracies in the WAVE IMPACT model as well as the uncertainty in the manner in which the input parameters are determined. This model factor is needed in a (semi-) probabilistic analysis of a dike section (WTI-2017 gedetailleerde toetsstap 2a).

As most experience was gained for asphaltic concrete (WAB), the quantification of the model factor will be done for this type of asphalt.

In order to calibrate the semi-probabilistic calculation, a full probabilistic analysis has been performed, on the basis of statistical distributions of the input parameters as well a statistical relation for the model factor. A statistical relation for the model factor has been obtained by considering several typical cases.

For open stone asphalt (OSA) no statistical analysis could be made, due to lack of data from assessments. Therefore, after a simple assessment, a next step is a specific assessment. No detailed assessment consisting of a semi-probabilistic calculation is possible. In the specific assessment an advanced (probabilistic) analysis can be performed, on the basis of a thorough field investigation. A guideline for this field investigation has been written recently, see [24].

However, the findings as to the model factor for asphaltic concrete (WAB) cannot directly be used for open stone asphalt, as the statistical distributions used were typical for WAB. In addition, other failure mechanisms can occur. For OSA that is directly placed on a geotextile on sand a failure plane in the sand under the open structure may develop, due to water pressures caused by wave attack. This means that the application of the WAVE IMPACT model alone is not enough. In several cases, especially in the wave attack zone, open stone asphalt is placed on a layer of lean sand asphalt. This prevents the occurrence of high pressures in the sand due to wave attack.

### 1.3 Reader's guide

In Chapter 1 the context and the aim of this report are given. In Chapter 2 the wave impact assessment model is described as well as some considerations as to the input parameters. In Chapter 3 the aspects influencing the safety with regard to the failure mechanism 'wave impact' are discussed, as well as an analysis to obtain the contribution of these aspects to the overall safety level (model factor). In Chapter 4 a value for the model factor  $\gamma_m$  is chosen, and also a statistical distribution for the model uncertainty factor "m" is derived by using estimates of the maximum en minimum partial factors. This information has been used by WTI-2017 cluster C to calibrate the partial safety factor  $\gamma_s^*$  that is related to the target safety level and the uncertainty in WAVE IMPACT input parameters. Also a method is proposed to estimate the outcome of the coming assessment for several representative cases, using the model factor  $\gamma_m$  and the partial safety factor  $\gamma_s^*$ , and on the basis of findings from previous assessments and experiences of water boards. In Chapter 5 conclusions and recommendations are given.



## 2 Description of WAVE IMPACT assessment (WTI-2017)

### 2.1 The WAVE IMPACT model

The theory for the WAVE IMPACT model is described in [1]. A short summary is given here. Figure 2.1 shows the schematisation in WAVE IMPACT for one wave attack.

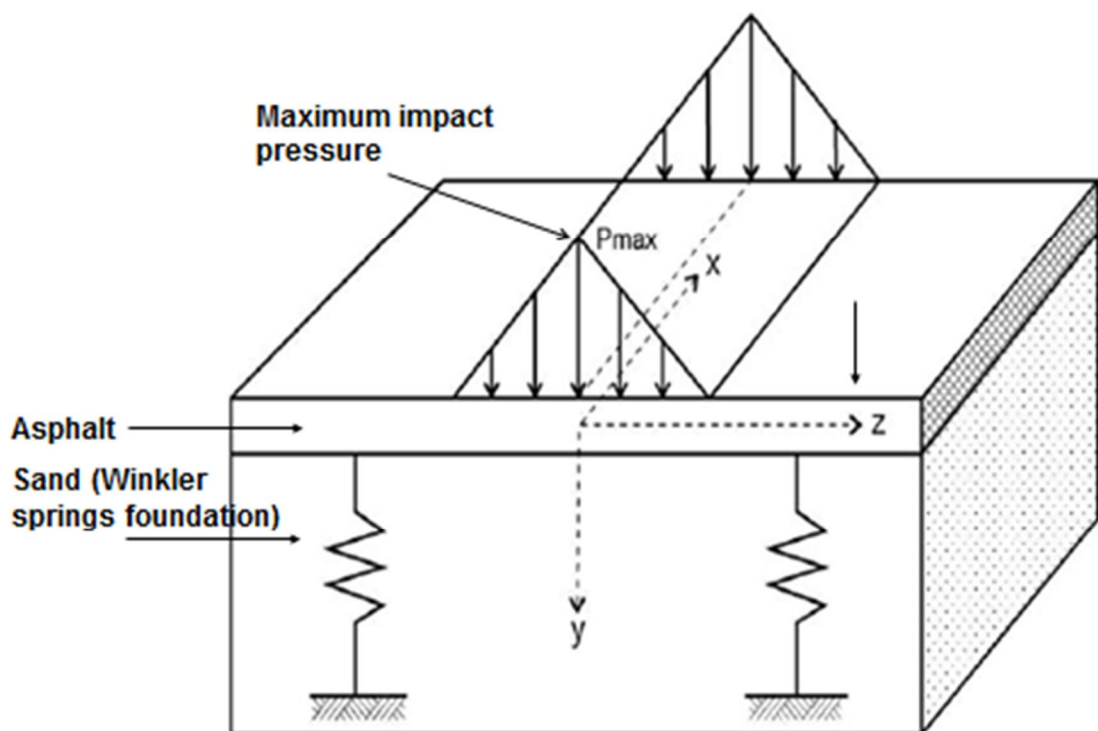


Figure 2.1 Schematisation in WAVE IMPACT of wave attack on an asphaltic revetment on a subsoil

#### Description of wave attack

On the basis of earlier Delta flume experiments the wave attacks during storm conditions can be described by means of a statistical model consisting of triangular wave loadings (see [1]). As the horizontal width of the waves is larger than 20 meter, the pressure distribution of the wave attacks is assumed to be two dimensional (plane strain). Furthermore, it is assumed that all waves are running perpendicularly to the dike surface. The statistical wave model (pressure distribution, wave impact point) was implemented in the software program WAVE IMPACT. The pressure distribution of one wave attack in this statistical model is assumed to be triangular with  $p_{max}$  as the maximum value of the triangle, see figure 2.1. The impact of a wave is then described by equation 2.1.

$$p_{max} = \tan(\alpha) / 0.25 \cdot \rho_w \cdot g \cdot q \cdot H_s \quad [\text{eq. 2.1}]$$

Where:

- $p_{max}$  = maximum pressure on dike surface (Pa);
- $\alpha$  = slope angle, reference is a slope of 1:4;
- $\rho_w$  = density of water ( $\text{kg/m}^3$ );
- $g$  = gravitational acceleration ( $\text{m/s}^2$ );
- $q$  = factor of impact (-);
- $H_s$  = significant wave height (m).

### Description of asphalt structure.

In Golfklap the bending stress at the underside of the asphalt is determined analytically, using a so-called Winkler spring foundation with a modulus of subgrade reaction  $c$ . The asphalt is considered as a plate with a constant thickness, behaving elastically with a modulus of elasticity  $E_a$  and a Poisson's ratio  $\nu_a$  (where it is assumed that the asphalt temperature is  $5^\circ\text{C}$  and the length of the wave impact is 0.1 sec, corresponding to 10 Hz; the parameters are strongly temperature dependent because of the visco-elastic nature of the asphalt. In the calculation method for the modulus of subgrade reaction the spreading of the load in the asphalt layer is taken into account, see [3]. This calculation method was based on the situation for a falling weight deflection measurement.

This implies that the subsoil is supposed to deform in a direction perpendicular to the slope, i.e. without a sideways spreading of the load (see figures 2.1 and 2.2). In figure 2.2 a comparison is made of the analytical approach and a finite element calculation for a load on an asphalt layer on a linear elastic subsoil. In the second case the load is spreading in the subsoil. This effect has to be taken into account when determining the safety of the WAVE IMPACT model.

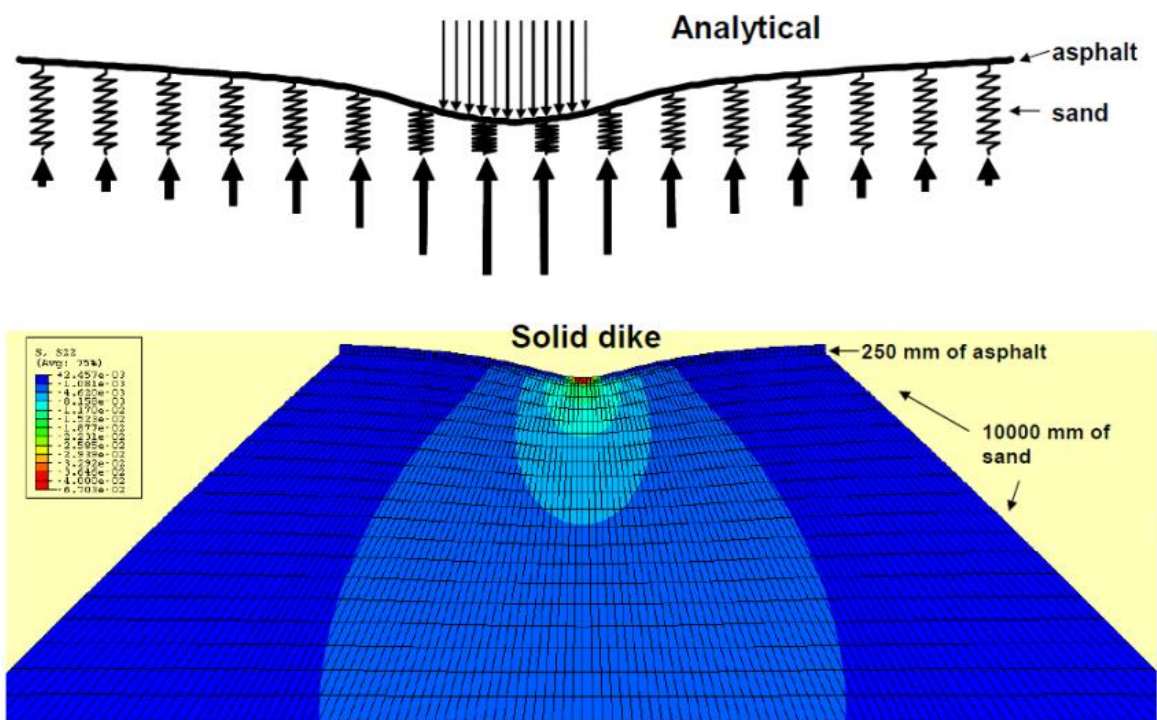


Figure 2.2 Comparison of deformation under wave attack for a Winkler spring foundation (above) and a solid (elastic) foundation (below). In reality the asphalt lies on a slope (1:2 to 1:5)



## 2.2 Failure in deterministic approach (previous safety assessment)

In this section the failure criterion is described that has been used in the past. In previous periodical safety assessments a deterministic failure criterion in case of fatigue was used, without using safety factors. In this approach the start of growth of a macro crack was considered to be failure, i.e. Miner's sum > 1, see below. For application in WTI-2017 this failure criterion has been modified, see section 2.5. A relation with the maximum allowable probability of failure is established by introducing the partial safety factor  $\gamma_s^*$ , that is needed for a semi-probabilistic approach.

In order to determine the allowable amount of fatigue of the asphalt the so-called Miner's rule is used, see equation 2.2.

$$\sum(n_i/N_{f,i}) = M \quad [\text{eq. 2.2}]$$

Where:

M = Miner's sum

i indicates the respective bending stress intervals

For a certain applied bending stress level i there is a maximum amount of allowable loadings  $N_{f,i}$  which is described by means of the so-called fatigue curve (see figure 2.6).

No failure occurs when  $M < 1$ , failure occurs when  $M > 1$ . At the moment of failure  $M=1$  a macro crack is initiated. When the loading continues, the fissure starts to grow. The amount of loadings during growth of the fissures up to crossing the total layer thickness is called the residual strength of the asphalt layer.

Figure 2.3 shows an example of the output from the WAVE IMPACT model. The wave impacts are different depending on the position across the slope, and therefore, the Miner's sum differs. The maximum Miner's sum across the slope is inserted in the failure criterion (Eq. 2.2).

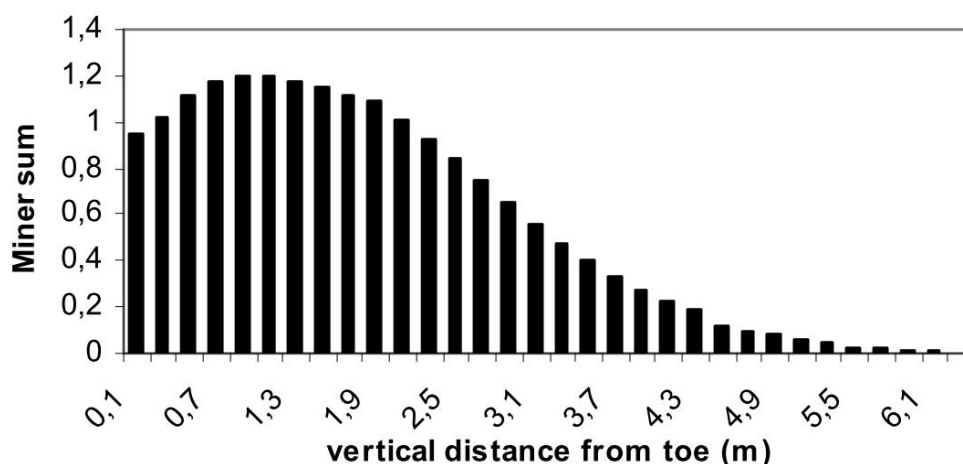


Figure 2.3 Output from the WAVE IMPACT model; the assessment is based on the maximum in Miner's sum (in this example  $M_{max} = 1,2$  at distance 1,3 m)

### 2.3 Input parameters

A periodic safety assessment for failure mechanism 1 (wave attack) is based on data from visual inspections, monitoring and laboratory testing of core samples. These are:

- Falling weight deflection measurements (FWD, see [6] and figure 2.4) to determine the stiffness of the asphalt layer and the subsoil (using data on layer thickness).
- Laboratory testing on small asphalt samples to determine the fatigue line (3 point bending tests, see [7] and figures 2.5 for the equipment and 2.6 for an example of a fatigue line).
- Ground Penetrating Radar measurements for determination of the layer thickness.
- Visual inspection to discover damages, cracks etc. (also reduction of layer thickness due to erosion and stripping).

For the assessment of the asphalt stiffness by means of falling weight deflection measurements the stiffness is calculated at 5 °C and 10 Hz, see [3]. These conditions are considered to be typical for a Dutch winter storm. The wave impact pulse takes order of 0.1 seconds, which corresponds to 10 Hz. In [3] it is prescribed to perform FWD-measurements in case the asphalt temperature is at maximum 15 °C. This is because the asphalt properties are largely temperature dependent and it is difficult to correct FWD-measurement values to 5 °C in case the measurement temperature is higher than 15 °C.

The assessment by WAVE IMPACT needs information about the fatigue line, i.e values for  $N_{f,i}$  as a function of the stress level. The fatigue line has the following form, see [7] and figure 2.6:

$$\log(N) = \beta(\log(\sigma_b/\sigma_0))^\alpha \quad [\text{eq. 2.3}]$$

Where:

N = maximum amount of allowable loadings

$\sigma_0$  = applied bending stress in the fatigue test (MPa)

$\sigma_b$  = flexural strength at one load repetition (MPa)

$\alpha, \beta$  = regression coefficients

$\log( )$  = common logarithm (base 10)

$\alpha$  and  $\beta$  are input parameters for WAVE IMPACT, as well as the 5% characteristic value for the flexural strength  $\sigma_b$ , see Table 2.1.

Based on of a large set of experimental data the following basic principles for the material model were established:

- The model should take into account the flexural strength at one load repetition. The fatigue line is curvilinear on a log-log scale.
- The model should be suitable to deal with a large variation in the test results. To reduce the variation,  $(\sigma_0/\sigma_b)$ , is used as the independent variable instead of  $\sigma_0$ . Variation in  $N_f$  given a  $\sigma_0$  can mostly be explained by the variation in  $\sigma_b$ . This method is known from fatigue curves for concrete pavements in road engineering.

In order to obtain a safe fatigue line, the 5% characteristic value for the flexural strength  $\sigma_b$  at one load repetition is inserted. The analysis of many practical cases indicates that the variation in the flexural strength now covers the uncertainty in the results of the fatigue tests as well. When using this fatigue line in practice, normally less than 5% of the results from the fatigue tests is on the left side of the fatigue curve (see figure 2.6).

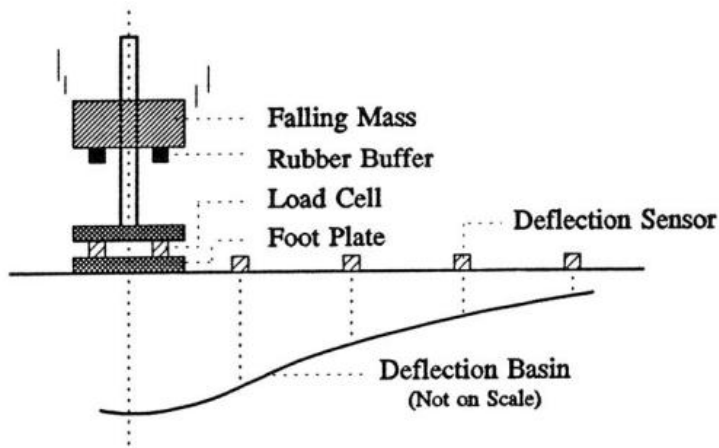


Figure 2.4 Principle of falling weight deflection test



Figure 2.5 Start of yielding of asphaltic concrete in 3 point bending test: a large crack has occurred (see top middle part of asphalt sample)

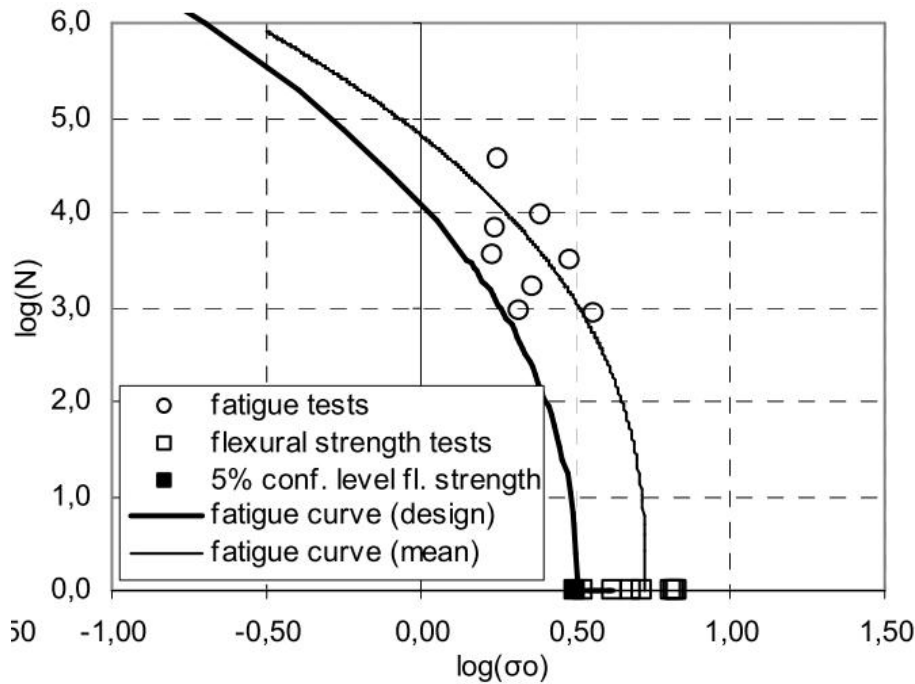


Figure 2.6 Fatigue line for Hondsbossche seawall: for a certain applied bending stress  $\sigma\sigma$  there is a maximum amount of allowable loadings  $N$ . For the design curve the 5% boundary for flexural strength has been inserted

Table 2.1 gives an overview of the input parameters needed for the WAVE IMPACT assessment model and the way they are determined. In [3] the procedure to determine these parameters is described. The stiffness and flexural strength of the asphalt are temperature en frequency dependent, as asphalt is a visco-elastic material.

Parameters	Amount of safety in parameters	Notes
Waterlevel + additions [m]	Q-variant, see [23]	For a series of probabilities of occurrence hydraulic boundary conditions are to be derived for a certain dike section. The water level varies during the storm.
Significant wave height $H_s$ [m] en average waveperiod $T_{mean}$ [sec]	Q-variant, see [23]	For a series of probabilities of occurrence hydraulic boundary conditions are to be derived for a certain dike section.
Storm duration	see [23]	Deterministic. Depends on probability of occurrence of the set of hydraulic conditions.
Modulus of subgrade reaction subsoil $c_{5\%}$ [MPa/m]	5% characteristic value from a cumulative frequency distribution based on at least 20 measurements per dike section	From Falling Weight Deflection tests, normally when the phreatic line is low.
Stiffness asphalt $E_{a95\%}$ [MPa]; Poisson's ratio $\nu_a = 0.35 = \text{default}$	95% characteristic value from a cumulative frequency distribution based on at least 20 measurements per dike section. Temperature $5^\circ\text{C}$ and frequency = 10 Hz. (*).	From Falling Weight Deflection tests, normally when the phreatic line is low.
Flexural strength asphalt $\sigma_{b,5\%}$ [MPa]	5% characteristic value from a lognormal distribution based on at least 8 borings per dike section; temperature = $5^\circ\text{C}$ ; loading speed 0.35 mm/s (*).	From 3 point-bending tests on small samples (fatigue test and flexural strength test on twin samples).
Regression coefficients fatigue line $\alpha, \beta$	average values	$\alpha$ and $\beta$ from a regression of fatigue test and flexural strength test data, see [7].
Thickness of asphalt layer $h_{5\%}$ [m]	5% characteristic value from a cumulative frequency distribution based on at least 100 measurements per dike section	In case the thickness is smaller, the Miner's sum is higher (for common thickness range)
Coordinates of lower and upper boundary of slope section	Slope angle is derived by interpolation.	In case parts of the slope section are steeper than the interpolation, this is unsafe.

Table 2.1 Choice of values for WAVE IMPACT input parameters, plus determination method

#### Correlation between input parameters

In the past, a number of investigations on dike sections were performed (see [8] and [16]) to establish the scales of spatial variation of the WAVE IMPACT input parameters such as:

- Asphalt layer thickness.
- Flexural strength of asphalt and fatigue properties asphalt (from tests on small samples).
- Dynamic stiffness moduli on small samples of asphalt.
- Results based on Falling Weight Deflection (FWD) tests (asphalt strain, asphalt stiffness, subsoil stiffness).

For individual points on the dike sections, there was no correlation between the stiffness data on small samples and the results from FWD-tests (figure 2.8). When comparing all the data per dike section for a series of dike sections, it was found that there was a weak correlation ( $R^2 = 0.41$ ) between the 95% characteristic asphalt strain (maximum strain at the bottom of the asphalt layer) obtained from FWD-tests (per dike section) and the 5% characteristic flexural strength  $\sigma_{b,5\%}$  (per dike section, from tests on small samples, see figure 2.7 (from [19])).

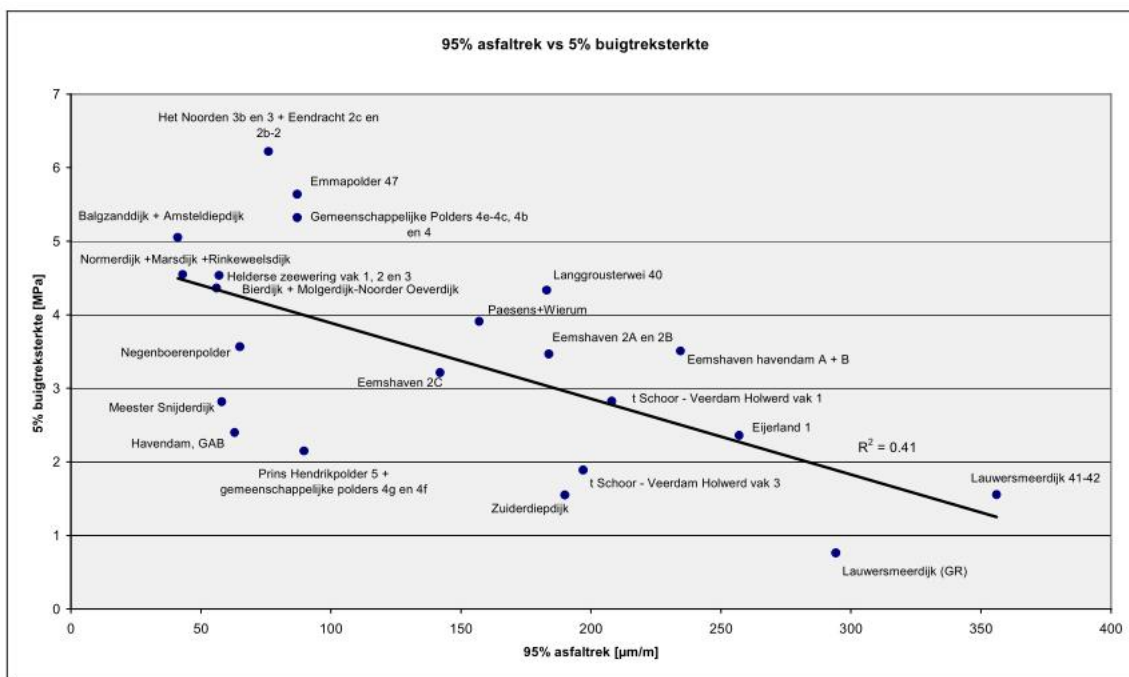


Figure 2.7 Relation per dike section between the 5% characteristic value of flexural asphalt strength and the 95% characteristic value of the asphalt strain with  $R^2=0,41$  (from [19])

The asphalt strain from FWD-tests is strongly related to the asphalt stiffness that is obtained from FWD-measurements (see [16]), where for the analysis of the asphalt stiffness the layer thickness values from radar measurements have been used. A 95% characteristic asphalt strain corresponds well with a 5% characteristic asphalt stiffness, see [16]. This implies that there is also a weak correlation between the 5% characteristic asphalt stiffness and the 5% characteristic flexural asphalt strength. The current safety assessment uses a 95% upper boundary for E-asphalt from FWD-tests per dike section. This is possibly too conservative: in case the asphalt stiffness is higher, the tensile stress is higher, which is unfavourable.

### Correlation length

Knowledge on the correlation length of the respective parameters is of importance for probabilistic calculations, in order to obtain a probability of failure for a dike section. The WAVE IMPACT safety assessment assumes that all material properties in the vertical direction are the same, which has to be accounted for as well.

In [8] it was found for a part of the Eemshaven dike that there is a correlation for the asphalt stiffness results from FWD-tests on a scale of several meters. In the horizontal direction (along the dike) the correlation was significantly less (a correlation length of up to 3 meters) than in the vertical direction (across the dike) (a correlation length of 8 meters). This

difference in correlation length can be explained by the construction process. At Eemshaven the asphalt was applied in batches and densified for parts with a width of about 3 meters and a length across the slope up to 20 meters.

In order to reveal the correlation length, the stiffness  $E_a$  was checked for extreme values that could be caused by observed irregularities in the structure, such as damages and reparation patches. In practice, the  $E_a$  values are not analysed in that detail, which means that the spreading in  $E_a$  is usually significantly higher (due to irregularities) than expected for the regular structure without damages. It is expected that damages should result in lower values for the FWD-stiffness modulus as compared to laboratory values on small samples ( $E_{dyn}$ ). However, this is often not the case, see figure 2.8 (taken from [16]).

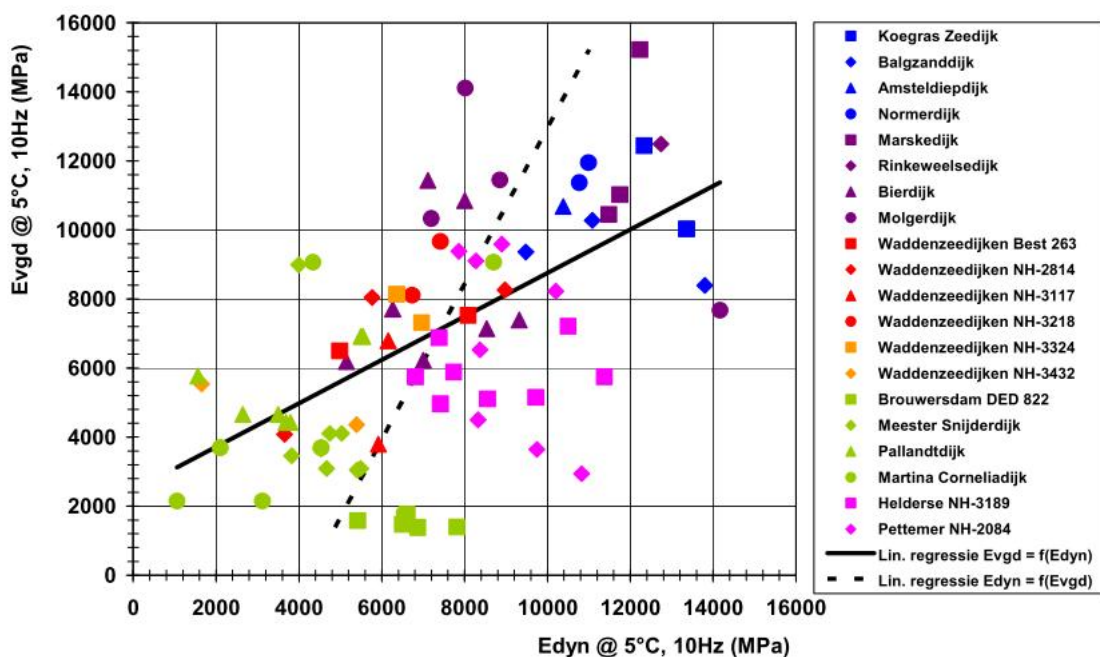


Figure 2.8 Relation per point between the asphalt stiffness ( $E_{vgd}$ ) from falling weight deflection tests (as calculated according to [3]) and the asphalt stiffness ( $E_{dyn}$ ) from tests on small samples for a series of locations (from [16])

The modulus of subgrade reaction is determined on the basis of the subsoil stiffness from the same FWD-tests (see [3]), normally without extra information on the condition of the subsoil. The calculation method for the modulus of subgrade reaction needs evaluation, see chapter 3. The observed variation in modulus of subgrade reaction is quite large.

There is no clear correlation between the modulus of subgrade reaction and the asphalt stiffness. It is advised to take as input for WAVE IMPACT de 5% lower boundary per dike section, which is common practice already, see [3].

As to the flexural strength, large variations on a small scale (decimetres) are possible, see [4]. As cracks can start to grow locally, these variations are of significance. Also local changes in thickness are of relevance, see section 3.5.

It is not well known yet on what scale the revetment fails under storm conditions. It is likely that the spatial distribution of parameters, such as the asphalt stiffness, layer thickness and the flexural strength play an important role. Up to now, it is assumed that the WAVE IMPACT

calculation (with the parameter determination as prescribed in the assessment guideline) is valid for one dike section of typical 1000 m length as a whole (as part of one construct contract). In future, it might be necessary to distinguish subsections within the dike section, with a dimension that corresponds to the scale of failure of the construction. This can be related to the spatial distribution of the parameters involved.

More research is needed on how the observed spatial variations can be averaged in the zone where damage due to wave attack is expected and also how safe values can be taken for the assessment. Also the FWD-analysis has to be evaluated; more data points per m<sup>2</sup> are needed and the derivation of the asphalt stiffness and subgrade modulus has to be evaluated.

In the calibration study, see [20], it has been assumed that the length of the independent equivalent reaches is 1000 m, that means that it has been assumed that the statistical distribution of the input parameters (as determined in the safety assessment) are representative for failure according to WAVE IMPACT of the whole dike section.

## 2.4 The WTI-2017 safety assessment steps

In the WTI-2017 assessment rules will be developed, using a stepwise assessment, see figure 2.9. The detailed assessment for asphalt under wave attack consists of a semi-probabilistic method, using the WAVE IMPACT model and the failure criterion as given in section 2.5, eq. 2.5. A fully probabilistic approach is needed to calibrate the safety factors. A fully probabilistic approach will not be part of the WTI-2017 assessment procedure in Ringtoets, however.

## Principle of safety assessment

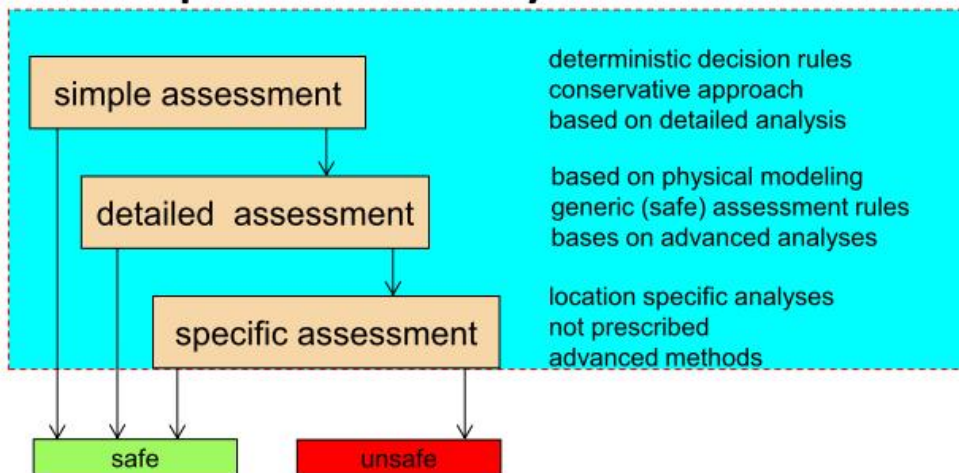


Figure 2.9 Stepwise safety assessment in WTI-2017

## 2.5 Modified failure criterion and safety factors

Up till now, the failure criterion was deterministic and based on the Miner's sum  $M$ . The most straightforward criterion for a semi-probabilistic calculation is to introduce two safety factors, i.e.  $\gamma_s$  and  $\gamma_m$  on the Miner's sum. Where  $\gamma_s$  accounts for uncertainty due to spatial variability in the horizontal direction and is related (by calibration) to the required safety level (probability of failure of a dike section), whereas  $\gamma_m$  accounts for uncertainty due to the limitations of the safety assessment with the model WAVE IMPACT.



For statistical reasons a logarithm of the Miner's sum was taken to derive a safety format, see [20]. The proposed limit state function for wave impact on asphalt dikes is (see [20]):

$$Z_A = -\log_{10}(m \cdot M) \quad [\text{eq. 2.4}]$$

Where:

m = the lognormal distribution of the model uncertainty factor.

M = Miner's sum

The first step in the calibration is to make a semi-probabilistic design using the representative values of the different parameters. The proposed safety format for the semi-probabilistic design is, see [20]:

$$\log_{10}(\gamma_m M) < -\gamma_s^* \quad [\text{eq. 2.5}]$$

Where:  $\gamma_s^* = \log(\gamma_s)$ ; Note: in [20] different symbols have been used.

Or

$$M \cdot \gamma_s \cdot \gamma_m < 1, \quad [\text{eq 2.6}]$$

$\gamma_s^*$  is dependent on the target probability (reliability index  $\beta$ ) and differs per safety standard. Also length effects are accounted for in this factor, see [20]. In the safety assessment this safety factor should be derived from the  $\beta$ - $\gamma_s^*$  - relations following from the calibration.

The model factor  $\gamma_m$  is the most probable value of the model uncertainty factor (see figure 4.1) which incorporates how well the WAVE IMPACT model predicts the asphalt resistance (model uncertainty).



### 3 Safety of WAVE IMPACT assessment

#### 3.1 Overview of aspects influencing safety

The following categories of aspects that influence the safety assessment by means of the WAVE IMPACT model have been identified:

1. limitations, choices and inaccuracies of WAVE IMPACT model itself:
  - a. Subsoil schematisation.
  - b. Schematisation of wave impact.
  - c. Number of significant wave loadings.
  - d. Assumption of uniform material parameters in the vertical direction.
  - e. Determination of slope angle in WAVE IMPACT (interpolation).
2. Uncertainty in the calculation of the Miner's sum (failure criterion).
3. Irregularities in the structure (for example: sudden changes in layer thickness).
4. Degree of saturation of the dike body (position of phreatic line).
5. Assumptions and uncertainties in the determination of the WAVE IMPACT input parameters.
6. Effect of (high) temperature.
7. Residual strength as to the growth of cracks after initial failure.

The reliability of the determination method of the input parameters has to be considered as well. It was found that the measurement accuracy is much less than the spatial variation [8]. In addition, no systematic errors were found.

These aspects have to be evaluated. In section 3.2 it is described how this can be done for the respective aspects one by one. In the subsequent sections the analysis for respective aspects 1 to 7 is described.

In Chapter 4 a trial semi-probabilistic assessment is proposed on the basis of knowledge from previous assessments and the results from the calibration of the safety factor. This is thought to be useful in order to judge whether the safety factors are realistic.

#### 3.2 How to assess the amount of safety in the WAVE IMPACT model

In this section the subsequent aspects (1 to 7 from section 3.1) that contribute as partial factors to the model factor  $\gamma_m$  are described.

##### Aspect 1a: subsoil schematisation

Calculations can be done in which the sensitivity of the Miner's sum  $M$  can be investigated for several typical cases.

As to the schematisation of the subsoil, a linking pin to values for  $M$  is the tensile bending stress level. The tensile stresses in the WAVE IMPACT model can be compared with values from finite element calculations, using a more realistic subsoil material model, see for example figure 2.2 for a comparison. Also the calculation method of the modulus of subgrade reaction  $c$  needs to be taken into account in this analysis.

##### Aspect 1b: schematisation of wave impact

For the schematisation of the wave impact, the sensitivity of  $M$  to changes in the factor of impact  $q$  (see eq. 2.1) can be investigated. Other aspects as to the statistical distribution for the width of the wave impact and the location of the impact point are treated in [9]. From this study follows that it is not straightforward to improve these aspects, especially a distinction in values for the breaker parameter was not possible on the basis of the data analysed.

**Aspect 1c: determination of the number of significant wave loadings**

From Delta flume experiments it is known that not all incoming waves give a significant wave attack. This effect largely depends on the breaker parameter. For a practical range for this breaker parameter a correction can be made.

**Aspect 1d: assumption of uniform material parameters across the dike.**

This assumption has to be related to the dimension of the zone of failure across the dike slope, which might be a few meters wide. The correlation length across the slope might be smaller than the width of the asphalt layer (for example for the asphalt stiffness it was found to be 8 meters (see [8]) as compared to an asphalt width of 20 meters). In this report it is discussed how the spatial variability can be taken into account.

**Aspect 1e: determination of slope angle in WAVE IMPACT (interpolation).**

A steeper slope leads to a higher wave impact pressure, see equation 2.1. The formula is applicable for slope angles between 1:3 and 1:8, see [1]. In the schematisation guide (for the WAVE IMPACT assessment) it will be prescribed how to make distinct sections across the slope in case the slope angle is not constant. This means that for all these distinct sections WAVE IMPACT calculations have to be performed. In case of a more or less horizontal berm, the slope angle will be given as a practical value that is to be derived from the slope beneath.

**Aspect 2: uncertainty in the calculation of the Miner's sum (failure criterion).** A sequence of a severe load followed by smaller loadings gives more damage to the revetment, than a sequence of smaller loadings followed by a severe load. In an actual situation this sequence in stress levels is not known, as the sequence in type and magnitude of wave attacks is not known. The calculation of the Miner's sum is just additive and does not take into account these sequence effects, which means that the current calculation might not be safe enough.

**Aspect 3: irregularities in structure**

These irregularities are sealings between subsections and (repaired) damages. These have to be judged visually, whether sand comes out or not. Other irregularities are local changes in layer thickness, due to the irregular bottom profile of the asphalt.

The effect of the irregular bottom asphalt surface might be investigated experimentally as an effect on the value for the flexural strength  $\sigma_b$ . This effect can be taken into account in a sensitivity analysis on the basis of the WAVE IMPACT model, giving an effect on the Miner's sum.

**Aspect 4 degree of saturation of the dike body (position phreatic line)**

Saturation of the subsoil has a considerable effect on the bearing capacity. This can be investigated numerically by using a routine within the MPM-code (Material Point Method), see [14] for preliminary results. In 1992 Deltaflume experiments were done, including tests with a high phreatic level in the subsoil, see [15]. From these findings a rough estimate of the effect on the Miner's sum will be made, by using the increase in strain that was found. This aspect will not be taken into account for the standard detailed assessment, in which it is specified as a requirement that the phreatic line is low enough. The case of a higher phreatic line will be part of a specific assessment, see figure 2.9.

**Aspect 5: assumptions and uncertainties in de determination of the WAVE IMPACT input parameters**

The determination method of the input parameters asphalt stiffness  $E_a$ , modulus of subgrade reaction  $c$  and layer thickness of asphalt  $h$  is evaluated in [4]. In [4] also the fatigue line is considered as to the testing conditions and the accuracy of these. In addition, the falling weight deflection measurement and its analysis are evaluated. In case systematic errors

occur, a correction factor is needed. The spatial spreading of the input values is taken into account in the calibration of the safety factor  $\gamma_s$ .

#### Aspect 6: effect temperature

During the winter period the temperature will often be different from the standard of 5 °C. This is covered by studying existing data from laboratory testing on asphalt at several temperatures.

#### Aspect 7: residual strength as to the growth of cracks after initial failure.

From the so called medium scale tests (on 40 year old asphalt on a sand bed) an estimation of this residual strength in term of number of loadings can be given, see [4].

### 3.3 Effect of limitations and inaccuracies of WAVE IMPACT model

In this section the contributions of the subsequent safety aspects as a partial factor to the model factor  $\gamma_m$  are treated.

#### 3.3.1 Subsoil schematisation (aspect 1a)

The effect of subsoil schematisation has been investigated in [21]. In order to determine the effect of the subsoil schematisation in the WAVE IMPACT model, several typical cases were defined for which a comparison was made between the Miner's sum from WAVE IMPACT and the Miner's sum from a more advanced approach

In the advanced approach finite element calculations were made in which a linear elastic material model was used for the sand bed as well as for the asphalt layer. In WAVE IMPACT the sand is schematised as a series of Winkler springs with a modulus of subgrade reaction  $c$ . A comparison of asphalt on a Winkler spring foundation and asphalt on a linear elastic subsoil is shown in figure 2.2.

Two default parameter sets were used, typical for asphalt of 30 years old and 50 years old.(table 3.1 and case 1 in table 3.2).

Parameters fatigue line	Fatigue line '30' (‘assessment line’)	Fatigue line '50' (‘design line’)
Flexural strength (5% boundary) $\sigma_{b,5\%}$ [MPa]	3.6	2.4
$\alpha$ [-] (regression coefficient in fatigue line)	0.5	0.5
$\beta$ [-] (regression coefficient in fatigue line)	4.8	5.4

Table 3.1 Parameters for the assessment fatigue line and design fatigue line

The parameters (fatigue line, asphalt stiffness and modulus of subgrade reaction) for the conservative cases were chosen as those taken for the derivation of the assessment graphs of WTI-2011 (with significant wave height versus layer thickness, see [10]). The first set of parameters were considered to be safe for asphalt concrete (WAB) of at most 30 years with a good initial quality (fatigue line '30'). The second set of parameters was considered to be safe for asphaltic concrete of at most 50 years with a good initial quality (fatigue line '50'). [11].

The sensitivity of the Miner's sum to the asphalt stiffness and the subsoil stiffness was investigated by defining additional cases. An overview of the parameters for these cases is given in Table 3.2.

Input parameters	Case 1	Case 2	Case 3	Case 4
Asphalt: stiffness (95% boundary) $E_{a95\%}$ [MPa]	5700	4000	7500	5700
Poisson's coefficient $\nu_a$ [-]	0.35			
Modulus of subgrade reaction (5% boundary) $c_{5\%}$ [MPa/m]	64			117.9
Corresponding stiffness of sand $E_s$	32.57			60
Layer thickness (5% boundary) $h_{5\%}$ [m]	0.14			
slope	1 :3			
$H_s$ [m]	2.9			
$T_m$ [s]; i.e. average wave period	5.96			

Table 3.2 Input parameters for WAVE IMPACT calculation for 4 cases, used in combination with the assessment fatigue line and design fatigue line (table 3.1)

For case 1 (see table 3.2)), the layer thickness for the fatigue line '30' case was adapted until the Miner's sum was just smaller than 1. This was done for a slope angle of 1:3. A Miner's sum of 0.906 results in this case. This layer thickness (0.14 m) has subsequently been taken the same for all cases.

For the factor of impact  $q$  a value of 6 was taken, i.e. almost the largest value from the statistical distribution of the factor of wave impact in the WAVE IMPACT model (see [1]).

In a first step, the asphaltic layer on sand was schematised in a finite element model, at first using Winkler springs for the sandy subsoil (as in WAVE IMPACT) in order to compare the tensile stresses at the underside of the asphalt from this numerical calculation with the outcome from the WAVE IMPACT model (on the basis of an analytical formula for the tensile stress). The agreement was fairly well, see [21]. This implies that the finite element model was made accurately enough, in order to use it for a more advanced subsoil material model.

In the second step, the subsoil in the finite element model was schematised as linear elastic sand. The stiffness of this sand was back calculated from the modulus of subgrade reaction and layer thickness from table 3.2, using the following formula (that is part of the guideline for acquisition of input parameters [3]):

$$C = \frac{E_s}{2a \cdot (1 - \nu^2)} \quad \text{eq. [3.1]}$$

with the following parameter values:

$c$  = modulus of subgrade reaction (MPa/m)

$E_s$  = stiffness of subsoil (from FWD-tests in MPa)

$\nu$  = Poisson's ratio of subsoil (for dry sand a value of 0.35 is taken)

$a$  = the radius of the foot plate of the FWD-apparatus (0,15 m) + thickness of asphalt layer (in order to account for spreading of the load due to the asphalt layer)

For  $c = 64$  MPa/m  $E_s = 32.57$  MPa.

In the third step the tensile stresses at the bottom of the asphalt layer were calculated by a series of finite element calculations in order to compare the outcome of WAVE IMPACT with the more advanced method. The tensile stresses at the bottom are relevant for the fatigue behaviour. Figure 3.1 gives an example of these calculated tensile stresses for a typical triangular wave load for the first case as given in table 3.1. Also the outcome from the WAVE IMPACT model is shown.

According to the WAVE IMPACT formula, the tensile stresses strongly depend on the value of  $z/H_s$ , with  $z$  = half the width of the base of the triangular wave load, and  $H_s$  = significant wave height, see figure 3.2. The values of  $z/H_s$  in the WAVE IMPACT model range from 0.05 to 0.75. This range was covered in the calculations, see [21].

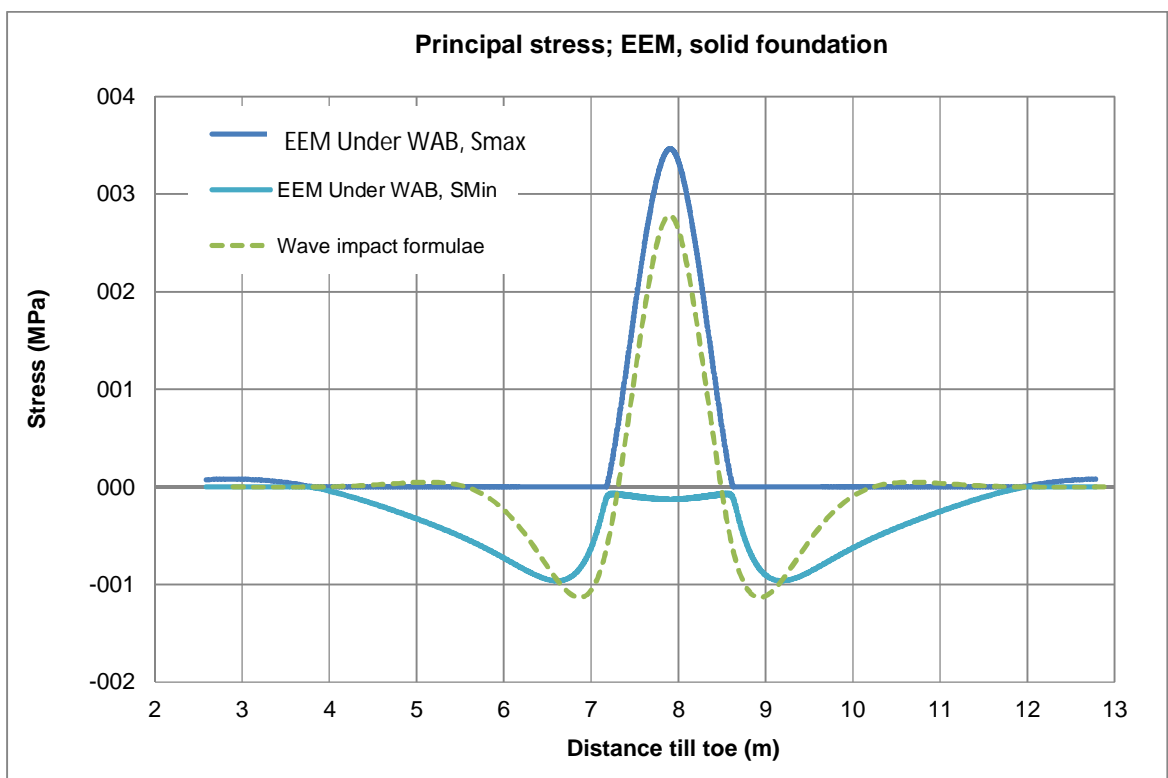


Figure 3.1 Comparison of tensile stresses for a linear elastic subsoil and those from the WAVE IMPACT formula, with  $z/H_s = 0.25$  (for the first case)

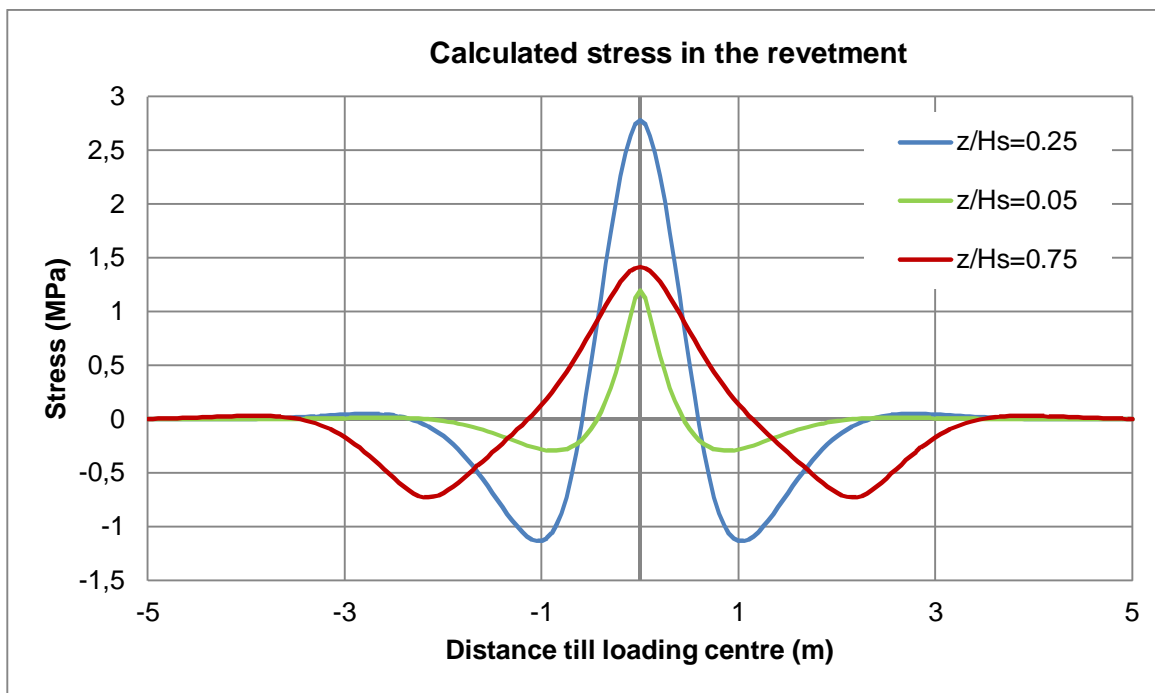


Figure 3.2 The tensile stress distribution (at the underside of the asphalt) from the WAVE IMPACT formula for 3 values of  $z/H_s$ , with  $z$  = half the width of the base of the triangular wave load (for the first case)

As a final aspect, the effect of the width of the wave load on the tensile stresses (at the underside of the asphalt) was investigated. In the finite element calculations, using a linear elastic subsoil, there appears a clear dependence of the tensile stresses on the width of the wave load. The values are significantly different from the results of WAVE IMPACT, as shown in figure 3.3 for the maximum tensile stresses, especially for large values of  $z$ , being the (half) width of the impact zone. A value above 100% means that the tensile stresses in the finite element calculation (using the linear elastic subsoil) are higher than in WAVE IMPACT.

Limited changes in tensile stress level can have a large effect on the Miner's sum, as the fatigue line is curved, i.e. in case the tensile stress increases up to the flexural strength the Miner's sum increases very much.



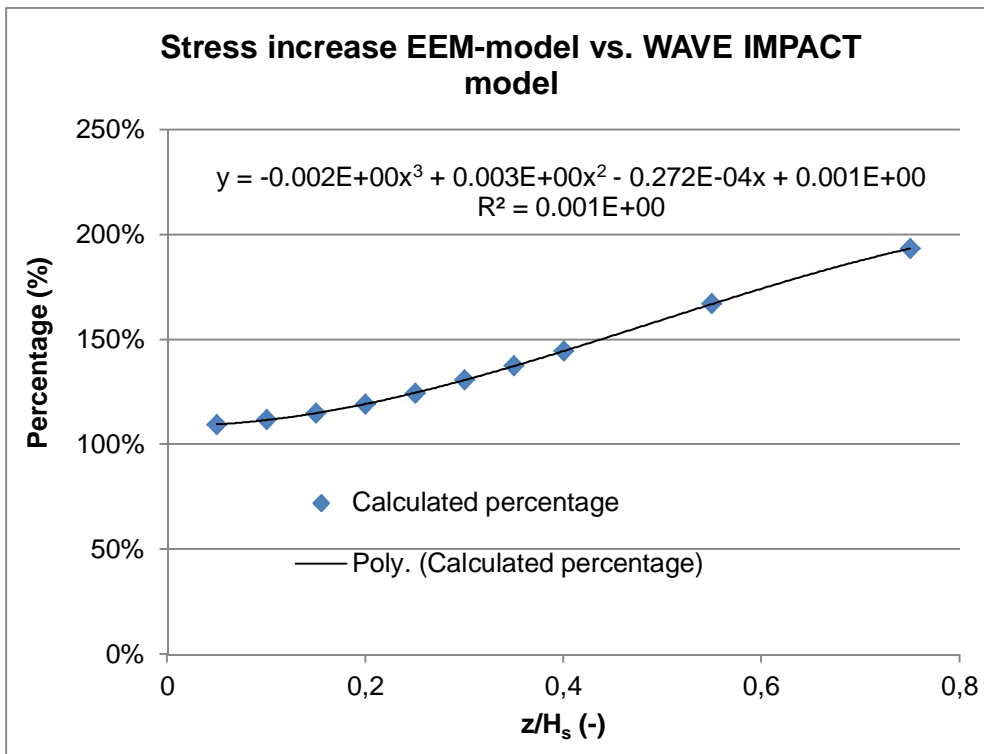


Figure 3.3 The quotient (in %) between the maximum tensile stresses for a linear elastic subsoil and those for the corresponding Winkler springs foundation (WAVE IMPACT model). These are the results for case 1 with the assessment fatigue line as given in Table 3.1. There is a strong dependence on  $z/H_s$

For all cases in table 3.1 a correction factor for the tensile stresses was determined as a function of  $z/H_s$ . This was done for several assumptions for the asphalt stiffness and stiffness of the subsoil, as well as for the assessment fatigue curve and with the design fatigue curve. The correction factor on the tensile stresses as a function of  $z/H_s$  was inserted in a calculation program (based on the WAVE IMPACT model) to obtain the Miner's sum for the respective cases. In table 3.3 the Miner's sum that is based on the finite element calculations has been compared with the Miner's sum from the WAVE IMPACT model, in order to derive a correction factor on the Miner's sum from the WAVE IMPACT approach. The last column in table 3.3 gives the quotient of this correction factor and the Miner's sum from the WAVE IMPACT model. This quotient has a smaller range than the correction factor, which indicates that there is a certain proportionality of the correction factor to the Miner's sum.

In the assessment Miner's sums ranging from about 0.2 to 1 are the most relevant according to  $M \cdot \gamma_s \cdot \gamma_m < 1$ , as this range is close to failure. Therefore, a range in Miner's sum between 0.2486 (for fatigue line '30',  $E_a = 5700$  MPa,  $E_s = 60$  MPa) and 1.054 (for fatigue line '50',  $E_a = 4000$  MPa,  $E_s = 32.57$  MPa) was taken to obtain the contribution to the model factor. Within this range the correction factor on the Miner's sum is roughly proportional to the Miner's sum, so only the boundary values were taken for further analysis.

	Ea and Es (Mpa)	M_wave impact	correction factor	corr factor/M_wave impact
assessment fatigue line	Ea=5700,Es=32.57	0,906	3,845	4,243929
	Ea=4000,Es=32.57	0,4198	2,274	5,416865
	Ea=7500,Es=32.57	1,7412	9,719	5,581783
	Ea=5700,Es=60	0,2486	1,461	5,876911
design fatigue line	Ea=5700,Es=32.57	5,351	14,4	2,691086
	Ea=4000,Es=32.57	1,054	5,45	5,170778
	Ea=7500,Es=32.57	21,119	15,67	0,741986
	Ea=5700,Es=60	0,477	1,67	3,501048

Table 3.32 An overview of the correction factor (4<sup>th</sup> column) needed on the Miner's sum from the WAVE IMPACT model

A first guess of the range in correction factor (factor in the model factor, see Chapter 4) is 5.45 (in case M = 1.054) to 1.461 (in case M = 0.2486).

### 3.3.2 Schematisation of wave impact (aspect 1b)

The factor of wave impact q (as given in equation 2.1) was determined from experimental results, see [1]. WAVE IMPACT applies in the calculation a lognormal distribution for q, derived from Figure 3.4. [12]. Figure 3.4 shows the cumulative probability distribution for the factor of wave impact ( $q = P_{max} / (\rho_w \cdot g \cdot H_s)$ ) for a series of experiments on a 1:4 slope, see

also equation 2.1. From this graph the probability distributions in graph 3.5 where derived. In the past), a conservative choice of this distribution was programmed in the WAVE IMPACT model. The choice to use the outer right boundary (with the highest q-values) in figure 3.4 was made to cover uncertainties in the schematisation that were not thoroughly analysed yet. The corresponding probability distribution in figure 3.5 is the red line (squares). For many practical cases this upper boundary is too conservative. A better choice is an average line in figure 3.4, which is a reduction of 20% on the q-values as compared to WAVE IMPACT. This corresponds with the blue line (diamonds).

This shift in probability distribution (see figure 3.5) has to be accounted for as a correction factor in the model factor on the Miner's sum.

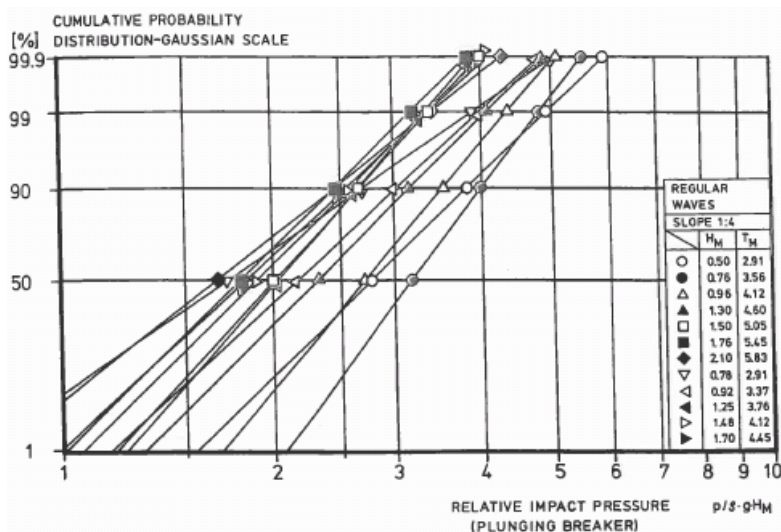


Figure 3.4 Cumulative probability distribution for the factor of wave impact for a series of laboratory tests with regular waves, see [12]

In order to determine the effect on the Miner's sum, two sets of calculations were performed:

- with the standard conservative values for  $q$  (the outer right curve in figure 3.5, as applied in WAVE IMPACT);
- and with the mean distribution in figure 3.5 (left curve, with a reduced  $p_{\max}$ ).

The same cases as in Table 3.1 and 3.2 were evaluated. Table 3.3 gives the results.

For example, for the first case as given in table 3.1, the Miner's sum with a reduced  $p_{\max}$  is 0.411 instead of 0.929 from WAVE IMPACT, which gives a correction factor of 0.44 on the Miner's sum.

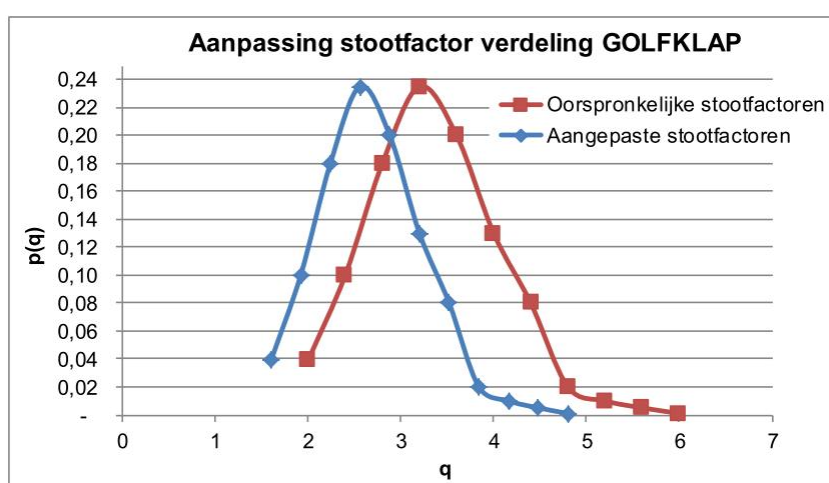


Figure 3.5 Shift in lognormal probability distribution for the factor of wave impact  $q$  from the conservative choice in WAVE IMPACT (on the right) to the mean one (on the left)

Case		Miner's sum M standard distribution of $q$	Miner's sum M mean distribution of $q$	Correction factor on M
Assessment fatigue line	Ea=5700 MPa, Es=32.57 MPa	0.929	0.411	0.44
	Ea=4000 MPa, Es=32.57 MPa	0.431	0.206	0.48
	Ea=7500 MPa, Es=32.57 MPa	1.791	0.725	0.40
	Ea=5700 MPa, Es=60 MPa	0.256	0.128	0.50
Design fatigue line	Ea=5700 MPa, Es=32.57 MPa	5.630	0.976	0.17

Table 3.3 Miner's sum  $M$  from calculations with the standard (conservative) distribution for the factor of wave impact  $q$  and  $M$  from calculations with an adapted (mean) distribution

From the results in Table 3.3 it can be concluded that a correction factor on  $M$  of 0.5 is desirable to make a more realistic estimate of the Miner's sum.

This has to be accounted for as a factor in the overall model factor, see Chapter 4.

### 3.3.3 Determination of number of significant wave loadings (aspect 1c)

The WAVE IMPACT model calculates the number of waves  $n$  for a certain level at the slope as follows:  $n = \text{time interval during which the still water level is at this height } (\Delta t) \text{ divided by the mean wave period } T_m$ , i.e.  $n = \Delta t/T_m$ . This implies that all incoming waves contribute to the Miner's sum.

Various investigations in the Delta flume have shown that only a part of the incoming waves cause significant wave attacks. This was determined including all positions on the dike slope. The effect strongly depends on the breaker parameter  $\xi_{op}$ , which is dependent on bed slope, wave height and wave period. Figure 3.6 from [9], for example, shows a relation between the breaker parameter and the number of significant wave attacks ( $N_{klap}$ ) divided by the total number of incoming waves ( $N$ ), i.e.  $N_{klap}/N$  (in full black symbols).

For the most common range in breaker parameter between 1 and 2 it follows that at most 78% of the incoming waves results in a significant attack, i.e.  $N_{klap} \leq 0.78 N$ .

This can be corrected for in the calculation of the Miner's sum, by multiplying the number of loadings  $n_i$  in equation 2.2 by a factor 0.78. This holds for all positions on the dike slope.

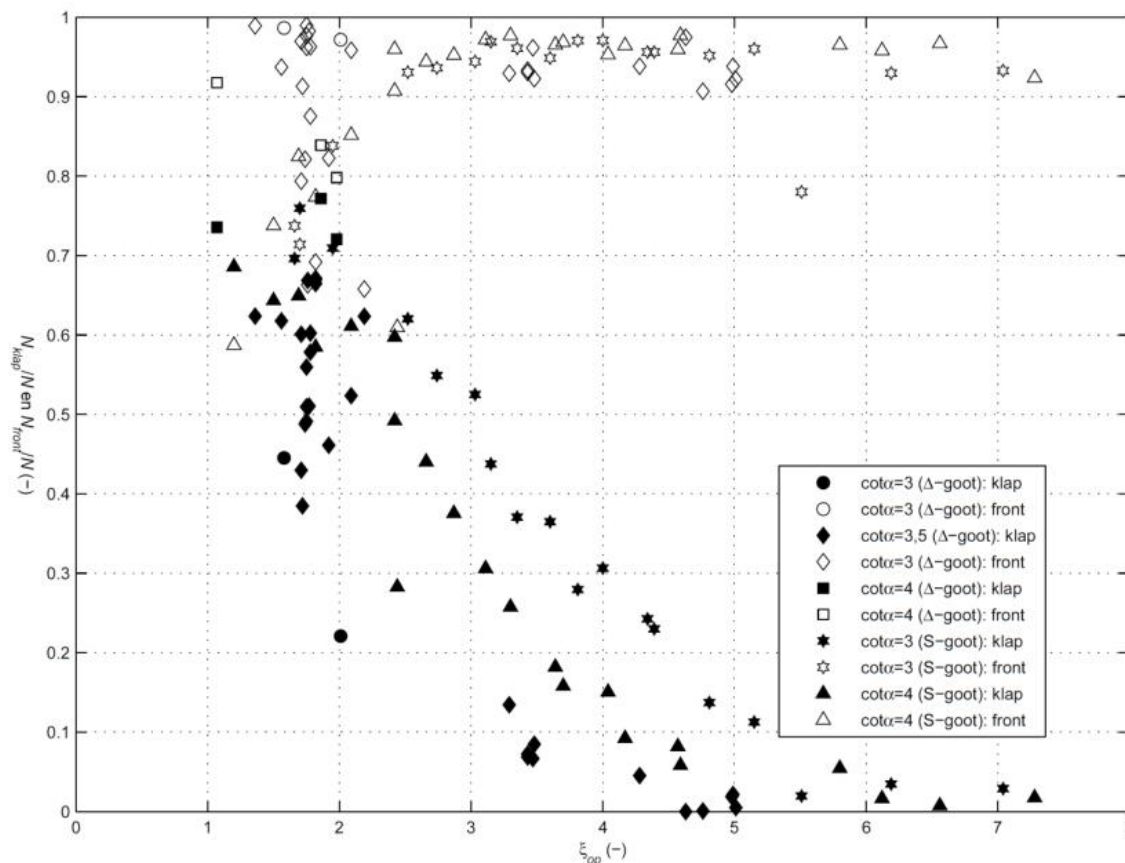


Figure 3.6 Number of significant wave loadings/number of incoming waves ( $N_{klap}/N$  in full symbols) as a function of the breaker parameter  $\xi_{op}$  see [9]

Since 0.78 is clearly an upper boundary, it is recommended to derive a statistical distribution for  $N_{klap}/N$  depending on the breaker parameter  $\xi_{op}$ . This could optimize the Miner's sum calculation to a lower value. The result can be integrated in a model factor probability distribution depending on the breaker parameter.

### 3.3.4 Assumption of uniform material parameters across the slope (aspect 1d)

In the WAVE IMPACT assessment Miner's sums are calculated along a line across the slope and the maximum value taken for the assessment, see section 2.2. By doing so it is assumed that all strength properties of the asphalt are the same across the slope (see section 2.3). The correlation length for these properties (up to 8 meters, see [8]) is smaller than the typical width of the asphalt revetment (about 20 meters). Thought has to be given to the dimension (across the slope) of the zone of failure, to find out whether this limited correlation length might be of relevance.

The zone of severe wave impact across the slope is a few meters wide. In the framework of the safety assessment, site investigation is executed in (or close to) this zone.

This implies that the input parameters are representative for the cross section zone of failure. Therefore it has been decided not to correct the Miner's sum for the effect of the limited correlation length (being at least 5 m or so), i.e. it is not taken into account in the model factor

$\gamma_m$ .

### 3.4 Effect of uncertainty in the calculation of the Miner's sum (failure criterion, aspect 2)

The failure criterion  $M = 1$ , is perhaps too simple. During a winter storm a severe load can cause crack damage and subsequent smaller loads (during the same storm) have more impact than in case of no crack damage. This means that the sequence in magnitude of wave loadings also determines the amount of allowable loadings. The definition of the Miner's sum makes no distinction as to this sequence.

As the fatigue line is bended (see figure 2.6 for an example), the severe loadings do result in a relatively higher contribution to the Miner's sum than smaller loadings. This implies that the number of allowed loadings is (much) less than what is common in road engineering, where a linear fatigue line is used. By implementation of the flexural strength as is done in the assessment of dike revetments the amount of allowable loadings at higher stresses is much less. It is thought that this adaptation to the fatigue line partially covers the risk in the sequence of loadings.

### 3.5 Effect of irregularities in the structure (aspect 3)

These irregularities are sealings between subsections and damages. These have to be judged visually, whether sand comes out or not. Other irregularities are local changes in layer thickness on a small (cm) scale, due to the irregular bottom profile of the asphalt. It is well known that in the vicinity of the top of a crack higher stresses occur, which might result in a sudden increase in crack depth and also in longer crack patterns in the planar direction. Also local stress concentrations in the mastic around the stones of the granular material in the asphalt mixture might be of influence on this crack propagation.

No experimental research concerning the effect of sudden changes in layer thickness on the fatigue behaviour, especially the flexural strength, has been conducted yet.

It is proposed to judge the effect of sudden changes in layer thickness in the light of residual strength of the asphaltic revetment. After cracks start to grow, it takes a significant time (hours) for the revetment to show an open crack or hole, through which sand can be transported (see also aspect 7 in section 3.9). It is estimated that the residual strength of the structure is large enough to cover the risk due to local stress concentrations. As the effect of both aspects (residual strength and local stress concentrations) is only roughly estimated, it is not possible to derive a contribution to the model factor for these aspects. Probably the effect of the combination of both aspects will be limited, and therefore it is not taken into account to assess the model factor.

### 3.6 Degree of saturation of dike body (aspect 4)

In 1992 Delta flume experiments have been conducted, including tests with a high phreatic level in the subsoil [15]. From these tests it appeared that in case the phreatic line is high, the strains are a factor 1.5 to 2 higher than in case the phreatic line is low (dry subsoil).

The effect of this increase in strain on the Miner's sum can be determined by using a linear fatigue line on the basis of strain, derived from experiments on small samples of asphaltic concrete (see figure 3.7 from [13]). This fatigue line is used and not the fatigue line based on tensile stresses, as in the Delta flume the tensile stresses were not measured.

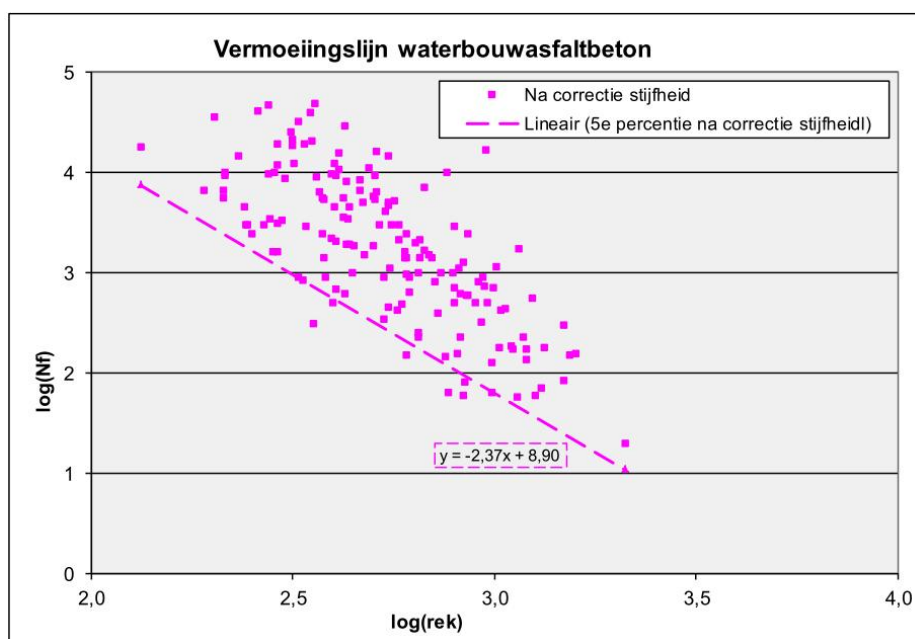


Figure 3.7 Data from fatigue tests (3 points bending) with a linear 5% percentile approximation of the relationship between the number of loadings until failure in terms of  $\log(N_f)$  and the strain in terms of  $\log(\text{strain})$ . This information concerns a number of dike sections in The Netherlands (from [13])

Figure 3.7 shows that an overall increase in strain results in a downward vertical shift of the fatigue line, i.e. the amount of allowable loadings  $N_f$  decreases. Table 3.5 shows some typical results:

Factor on strain	Strain [ $\mu\text{m}/\text{m}$ ]	$N_f$	Correction factor
1 (unchanged)	316	944	
1.5	474	361	2.6
2	632	183	5.2

Table 3.4 Decrease of the number of allowable loadings until failure  $N_f$  as a function of strain for an increase in strain

From these findings it follows that the Miner's sum has to be multiplied by at least a factor 2.6 in case the dike body has a high phreatic line. There is little experimental evidence to be sure about this factor. Preliminary numerical calculations with the MPM-code have been made [14] but these have not led to definite conclusions yet.

Since too much uncertainty exists with respect to the effects of a high phreatic line, this correction will not be included in the model factor for the assessment on a detailed level (see

figure 2.7). For the standard assessment it will be required that the phreatic line in the dike body is low. This requirement will be part of the safety assessment. In case the phreatic line is high a specific assessment is prescribed (see figure 2.9).

### 3.7 Assumptions and uncertainties in de determination of the WAVE IMPACT input parameters (aspect 5)

No systematic errors were found, see [8].

Therefore, no correction of the Miner's sum is needed, i.e. the partial factor on  $\gamma_m$  is 1.

The spatial spreading of the input values is taken into account in the calibration of the safety factor.

### 3.8 Effect of (high) temperature (aspect 6)

The asphalt stiffness and the fatigue line are determined for 5 °C. The temperature range during the winter storm period is 0 to 15 °C. A higher temperature results in a lower value of the stiffness, see [18]. In case the temperature is 15 °C, the stiffness of the asphalt is much lower (40% to 60% decrease), which implies that the asphalt bends more easily. It was found that tensile stresses are much lower (see [22]). Assessments reveal that a temperature of 5 to 7 °C is not uncommon [19], and even frozen asphalt was observed. This implies that for safety reasons it is not safe to correct the stiffness  $E_a$  for temperatures different from 5 °C.

The fatigue line is strongly influenced by the value of the flexural strength. It is known from experimental results that when the temperature increases by 10 °C from 5 °C to 15 °C a decrease of order of 10% in flexural strength occurs [17]. The asphalt temperature during the winter storm period will normally be lower than 15 °C- however, it has not been monitored that much- whereas the standard flexural strength laboratory test is performed at 5 °C. Thus, a shift of 10 °C is a safe assumption to deal with.

Table 3.6 shows the changes in Miner's sum for the respective cases, in case the flexural strength is decreased by 10%.

Case		Miner's sum M standard $\sigma_b$	Miner's sum M standard $\sigma_b \cdot 0,9$	Correction factor
Assessment fatigue line	Ea=5700 MPa, Es=32.57 MPa	0.929	1.433	1.54
	Ea=4000 MPa, Es=32.57 MPa	0.431	0.630	1.46
	Ea=7500 MPa, Es=32.57 MPa	1.791	2.983	1.67
	Ea=5700 MPa, Es=60 MPa	0.256	0.363	1.42
Design fatigue line	Ea=5700 MPa, Es=32.57 MPa	5.630	14.923	2.65

Table 3.5 The effect of 10% decrease in flexural strength on the Miner's sum

From Table 3.6 it follows that the Miner's sum increases with a factor 1.42 to 2.65.

In case the Miner's sum is < 1 this range is 1.42 to 1.54. It is desirable to use this last range, as it is expected that the new assessment rule implies that the revetment will be surely unsafe for a Miner's sum larger than 1. Thus, the partial factor to be implemented in the overall model factor  $\gamma_m$  ranges from 1.42 to 1.54. This is an estimate, as a limited number of cases have been evaluated.

### 3.9 Residual strength as to the growth of cracks after initial failure (aspect 7)

From the medium scale experiment 5 on 40 year old asphalt follows an 2.5 cm increase in crack depth within about 30 minutes (i.e. to one half of the 5 cm thickness of the asphalt in this test), see [4].

In this case the crack depth was at its theoretical maximum (i.e. at one half of the layer thickness in case of loading at the zone where the crack pattern occurred), which might imply that this maximum depth was reached in a shorter time, say 10 minutes.

From the measurements it is not very clear at what time the crack started to grow.

A time of 30 minutes amounts to 180 loadings, using the loading interval of 10 seconds.

There is only one observation of a growing crack available. For newly made asphalt, no cracks were detected in the medium scale tests, see [4].

An estimation of the effect of an increase of 180 in the amount of allowable loadings  $N_f$  can be derived from Table 3.5. In this table an increase in  $N_f$  from 183 to 361 results in a factor 2 reduction in Miner's sum.

In reality, the growth of cracks up to the asphalt surface might take longer (as the layer is at least 15 cm thick), and it takes even longer until a hole or open crack occurs.

In section 3.6 the effect of irregularities in the asphalt structure is described. This effect is considered of significant importance.

It is estimated that the residual strength of the structure is large enough to cover the risk due to local stress concentrations. As the effect of both aspects (residual strength and local stress concentrations) is only roughly estimated, it is not possible to determine a contribution to the model factor for these aspects. Probably the effect of the combination of both aspects will be limited, and therefore it is not taken into account to assess the model factor.



## 4 Assessment of probability distribution for the WAVE IMPACT model factor

In section 4.1 an overview of the partial factors contributing to the model factor is given. In section 4.2, the minimum and maximum value of the model factor  $\gamma_m$  are determined and a statistical distribution for the model uncertainty factor “m” is obtained. From this distribution for “m”, a value for  $\gamma_m$  is chosen.

### 4.1 Overview of partial factors in the model factor $\gamma_m$

Table 4.1 gives an overview of all partial factors and the judging of the respective aspects contributing to the safety.

aspect	partial factor (range)	notes
1a. subsoil schematisation	5.45 (in case M_wave impact = 1.054) to 1.461 (in case M_wave impact = 0.2486)	correction with respect to linear elastic subsoil for M_wave impact < 1 and $\approx 1$ .
1b. schematisation of wave impact	0.5 (in case M_wave impact smaller than 1)	a mean distribution for the factor of wave impact is taken instead of the WAVE-IMPACT calculation
1c. number of significant wave loadings	0.78	based on Delta flume experiments
1d. uniform material parameters in vertical	1	In agreement with choice for horizontal independent section of 1000 m
1e. changes in slope angle	1	Will be treated in schematisation guideline: take separate slope sections
2 uncertainty Miner's sum calculation	1	bended fatigue line increases safety as to sequence in strength wave attacks
3 irregularities in structure	--	Will be covered by aspect 7.
4 degree of saturation of dike body	2.6 to 5.2	will not be taken into account for standard detailed assessment, so not to be implemented in $\gamma_m$ .
5 input parameter determination	1	no systematic errors, no correction needed
6 effect of higher temperature	1.54 (in case M_wave impact = 0.906) to 1.42 (in case M_wave impact = 0.2486)	correction on the flexural strength for the risk of a higher temperature than 5 °C.
7 residual strength	--	will cover negative effect of aspect 3

Table 4.1 Overview of the partial factors contributing to model factor  $\gamma_m$  for the respective safety aspects.

## 4.2 Choice of statistical distribution for “m” and a choice for model factor $\gamma_m$ .

To obtain a minimum value for  $\gamma_m$  the following values for the partial factors are taken, see Table 4.2:

aspect	partial factor (range)
1a. subsoil schematisation	1.461 (in case M_wave impact = 0.2486)
1b. schematisation of wave impact	0.5 (in case M_wave impact smaller than 1)
1c. number of significant wave loadings	0.78
1d. uniform material parameters in vertical	1
1e. changes in slope angle	1
2 uncertainty Miner's sum calculation	1
3 irregularities in structure	--
4 degree of saturation of dike body	not included
5 input parameter determination	1
6 effect of higher temperature	1.42
7 residual strength	--
MULTIPLICATION $\gamma_m \min$	0.809

Table 4.2 The minimum value for the model factor  $\gamma_m$

To obtain a maximum value for  $\gamma_m$  the following values for the partial factors are taken, see Table 4.3:

aspect	partial factor (range)
1a. subsoil schematisation	5.45 (in case M_wave impact = 1.054)
1b. schematisation of wave impact	0.5 (in case M_wave impact smaller than 1)
1c. number of significant wave loadings	0.78
1d. uniform material parameters in vertical	1
1e. changes in slope angle	1
2 uncertainty Miner's sum calculation	1
3 irregularities in structure	--
4 degree of saturation of dike body	not included
5 input parameter determination	1
6 effect of higher temperature	1.54
7 residual strength	--
MULTIPLICATION $\gamma_m \max$	3.27

Table 4.3 Table 4.3 The maximum value for the model factor  $\gamma_m$

Next, a statistical distribution for the model uncertainty factor “m” has to be derived, which can be done on the basis of the minimum and maximum values for  $\gamma_m$  as given in tables 4.2 and 4.3. Use has been made of a lognormal distribution for the model uncertainty factor, as this is in accordance with the safety format in equation 2.5. The resulting probability density function “m” is given in figure 4.1.

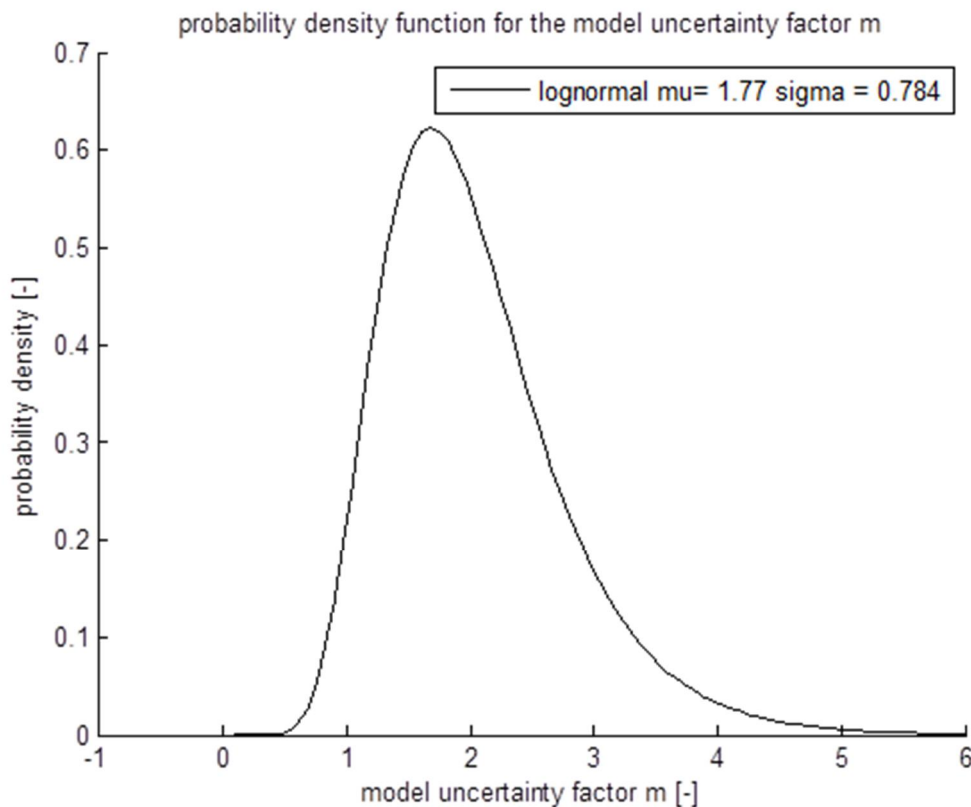


Figure 4.1 Probability distribution “m” (type: lognormal) for the I model factor  $\gamma_m$ .

This distribution was obtained as follows:

- The natural logarithm “ln” is taken of maximum and minimum values for  $\gamma_m$  (3.27 and 0.809 respectively), resulting in  $\ln(\gamma_m \text{ min}) = -0.212$  and  $\ln(\gamma_m \text{ max}) = 1.185$
- $\ln(\gamma_m \text{ min})$  and  $\ln(\gamma_m \text{ max})$  are considered to be the 5% and 95% characteristic values of a lognormal distribution (with an infinite number of observations)
- From these characteristic values the standard deviation  $\sigma_{\ln}$  is obtained from:  
 $\ln(\gamma_m \text{ max}) - \ln(\gamma_m \text{ min}) = 2 \cdot 1.645 \cdot \sigma_{\ln}$ , which gives  $\sigma_{\ln} = 0.42$
- The expectation (mean)  $\mu_{\ln}$  follows from:  $\mu_{\ln} = \ln(\gamma_m \text{ min}) + 1.645 \cdot \sigma_{\ln} = 0.48$
- From  $\mu_{\ln}$  and  $\sigma_{\ln}$   $\mu$  and  $\sigma$  for the corresponding normal distribution can be obtained by means of equations 4.1 and 4.2. It follows:  $\mu = 1.77$  and  $\sigma = 0.784$ .

$$\mu = \exp\{\mu_{\ln} + 0.5 \cdot \sigma_{\ln}^2\} \quad \text{eq. 4.1}$$

$$\sigma = \mu \cdot \sqrt{\exp(\sigma_{\ln}^2) - 1} \quad \text{eq. 4.2}$$

By calibrating (see [20]), a relation between the required amount of safety (index  $\beta$ ) and  $\gamma_s$  will be obtained, using the statistical distribution for “m” as shown in figure 4.1 in a monte-carlo based fully probabilistic analysis (see [20]). Part of this calibration is that a choice for  $\gamma_m$  has to be made. It is decided that in the semi-probabilistic assessment (rule M·  $\gamma_s \cdot \gamma_m < 1$  is safe, see section 2.5), the mean value  $\mu$  from the distribution for “m” will be used, i.e.  $\gamma_m = 1.77$  is taken.

The reason for this is that: from Table 4.1 it follows that especially the subsoil partial factor depends on the value of the Miner’s sum, i.e. a larger Miner’s sum gives a higher partial factor. Values for a Miner’s sum up to 1 have been taken into account. It is expected that application of the assessment rule (rule M·  $\gamma_s \cdot \gamma_m < 1$  is safe) will result in critical values for the Miner’s sum of the order of 0.1 to 0.5. Therefore a value for  $\gamma_m$  equal to the upper boundary for  $\gamma_m$  (at  $M = 1.054$ ) is too conservative.

It is advised to do a sensitivity analysis as to the probability of failure for a typical dike section with respect to the choice of  $\gamma_m$  (as a part of the final calibration).

#### 4.3 Application for a set of representative cases: trial safety assessment

For the aspects 1 to 7 as mentioned in section 3.1 choices have been made on how to determine or estimate the amount of safety. This was done for each aspect, one by one, and the total contribution to the model factor was determined. After doing so, a final judgement of the amount of safety for all aspects together is desirable.

In this paragraph a method is proposed to estimate the outcome of the coming assessment for several representative cases, using the model factor  $\gamma_m$  and the partial safety factor  $\gamma_s$ . This has to be done on the basis of findings from previous assessments and experiences of dike managers.

Table 4.4 gives a summary of a typical trial assessment. The results in Table 4.4 7<sup>th</sup> column can be compared with the 2<sup>nd</sup> column, which is based on engineering judgement, maintenance history, and results from previous assessments. Column 3 shows the Miner’s sum from previous assessments.

The relation between the required amount of safety (index  $\beta$ ) and  $\gamma_s$  (from the calibration, see[20]) will be used to obtain values for a set of representative cases.

On the basis of the values for  $\gamma_m (=1.77)$  and  $\gamma_s$  (different per case) and with the new hydraulic boundary conditions, it can be investigated what assessment results might be obtained in future for a series of practical cases, see table 4.5.

The cases have a Miner’s sum ( $M_{\text{WAVE IMPACT}}$ ) from previous assessment ranging from 0.003 to 467, see last column in Table 4.5. The ones smaller than 1 are the most relevant. It is recommended to extend the evaluation to the assessment results for the mechanism “material transport”, as this failure mechanism is related to the quality of the revetment as well.

Also the experiences on the amount of maintenance needed have to be taken into account.

Cases	Judgement: -from previous assessments; also on other failure mechanisms -info from water boards (maintenance history)	Minersum M_old from previous safety assessment: M-old < 1 is safe	Choice of $\gamma_s$ for respective cases, depending on norm and asphalt quality criterion; use will be made of $\gamma_m = 1,77$	New hydraulic boundary conditions at "toetspeil" (highest water level for norm)	Minersum from WAVE IMPACT model, using new hydraulic boundary conditions and other input from previous safety assessments	New assessment (semi-probabilistic) $\gamma_s \cdot \gamma_m \cdot M < 1$ YES or NO
1	Very safe/very unsafe/doubt					YES or NO
2 etc.	Very safe/very unsafe/doubt					YES or NO

Table 4.4 Trial assessment for the failure mechanism WAVE IMPACT (proposal to be used in future test assessment)

The cases to be considered are given in table 4.5.

Locatie	dijknaam	Kilometrering (m)		lengte vak (m)	MINER
Dijken Groningen	Negenboerenpolder	74000	82000	8000	0,051
Waddenzeedijk te Texel (NH-2814)	Prins Hendrikpolder	5700	6200	500	156
Waddenzeedijk te Texel (NH-2814)	Gemeenschappelijke Polders	6200	7200	1000	81,5
Waddenzeedijk te Texel (NH-2814)	Gemeenschappelijke Polders	7200	8700	1500	29,4
Waddenzeedijk te Texel (NH-3117)	Gemeenschappelijke Polders	10250	12400	2150	0,006
Waddenzeedijk te Texel (NH-3117)	Gemeenschappelijke Polders	13600	14600	1000	0,006
Waddenzeedijk te Texel (NH-3218)	Gemeenschappelijke Polders	15000	16800	1800	0,015
Waddenzeedijk te Texel (NH-3324)	Het Noorden	17100	18900	1800	0,322
Waddenzeedijk te Texel (NH-3324)	Het Noorden	18900	20300	1400	0,104
Waddenzeedijk te Texel (NH-3432)	Eendracht	20400	22000	1600	0,036
Waddenzeedijk te Texel (NH-3432)	Eendracht	22000	23700	1700	0,11
Waddenzeedijk te Texel (NH-3432)	Eijerland	24100	25400	1300	467
Waddenzeedijken (bestek NH 4264)	Balgzanddijk	9700	12500	2800	0,092
Noordzeedijken Noord-Holland	Helderse zeevering	0	1000	1000	0,003
Dijken Goeree	Zuiderdiepdijk	4200	6200	2000	0,829
	Lauwersmeerdijk				30

Table 4.5 A selection of cases to be considered for the evaluation of the new assessment.



## 5 Conclusions and recommendations

### 5.1 Conclusions

The following categories of aspects that influence the safety assessment by means of the WAVE IMPACT model have been identified:

1. Limitations, choices and inaccuracies of the WAVE IMPACT model itself:
  - a. Subsoil schematisation.
  - b. Schematisation of wave impact.
  - c. Number of significant wave loadings.
  - d. Assumption of uniform material parameters in the vertical direction.
  - e. Determination of slope angle in WAVE IMPACT (interpolation).
2. Uncertainty in the calculation of the Miner's sum (failure criterion).
3. Irregularities in the structure (for example: sudden changes in layer thickness).
4. Degree of saturation of the dike body (position of phreatic line).
5. Assumptions and uncertainties in the determination of the WAVE IMPACT input parameters.
6. Effect of (high) temperature.
7. Residual strength as to the growth of fissures after initial failure.

For the aspects 1 to 7 as mentioned in section 3.1 choices have been made on how to determine or estimate the amount of safety. This was done for each aspect, one by one, and next the total contribution to the model factor was determined.

A lognormal probability distribution "m" was constructed by using the minimum and maximum factors for all aspects contributing to safety. From "m" the model factor  $\gamma_m$  has been obtained, being its expectation value  $\mu = 1.77$ . The standard deviation is  $\sigma = 0.784$ .

After doing so, a final judgement of the amount of safety for all aspects together is still desirable.

In paragraph 4.3 a method is proposed to estimate the outcome of the coming assessment for several representative cases, using the model factor  $\gamma_m$  and the partial safety factor  $\gamma_s$ .

### 5.2 Recommendations

More research is needed on how the observed spatial variations can be averaged in the zone where damage due to wave attack is expected.

Also the FWD-analysis to obtain the asphalt stiffness and the stiffness of the subsoil has to be evaluated.

It is recommended to derive a statistical distribution for the number of significant wave attacks ( $N_{klap}$ ) divided by the total number of incoming waves ( $N$ ), i.e.  $N_{klap}/N$ , depending on the breaker parameter  $\xi_{op}$ . This can be integrated in a model factor probability distribution depending on the breaker parameter.

It is advised to do a sensitivity analysis as to the probability of failure for a typical dike section with respect to the choice of  $\gamma_m$  (as a part of the final calibration).

It is recommended to perform a trial safety assessment to estimate the outcome of the coming assessment for several representative cases, using the model factor  $\gamma_m$  and the

partial safety factor  $\gamma_s$ . This has to be done on the basis of findings from previous assessments and experiences of water boards. A selection of several representative cases is given, that can be used to perform such an assessment.

It is recommended to include the mechanism “material transport”, in the trial safety assessment as well, as this failure mechanism is also related to the quality of the revetment. Also the experiences as to the amount of maintenance needed have to be taken into account.



## 6 References

- [1] Paper *GOLFKLAP a model to determine the impact of waves on dike structures with an asphaltic concrete layer*. A.K. de Looff, R. 't Hart, C. Montauban, M.F.C. van de Ven. ICCE 2006, San Diego, September 3, 2006.
- [2] Rapport *GOLFKLAP voor mechanismebibliotheek*, R. 't Hart, Deltares juli 2014, kenmerk 1207811-015-HYE-0038.
- [3] *Werkwijzebeschrijving voor het uitvoeren van een gedetailleerde toetsing op golfklappen op een bekleding van waterbouwasfaltbeton Versie 4*, maart 2011.
- [4] Report *Validation of WAVE IMPACT assessment, based on an analysis of experimental results; WTI-product 5.14, asphaltic revetments*. Deltares (concept, December 2014) report 1209437-021-HYE-0010.
- [5] Rapport *Beschrijving veiligheden voor toetsspoor Golfklap asfaltdijkbekledingen; evaluatie van WTI-2011*, Deltares juli 2014, kenmerk 1207811-015-HYE-0041.
- [6] Paper *Valgewichtdeflectiemetingen op asfaltdijkbekledingen*  
Rien Davidse & Arjan K. de Looff KOAC•NPC, Martin F. C. van de Ven, TU Delft CROW Infra 2012.
- [7] Paper *Resistance of aged asphalt concrete to wave attack*, de Looff, Arjan K., Martin F.C. van de Ven, Robert 't Hart, 2011, Proceedings of the Coastal Structures 2011 conference, Yokohama.
- [8] Rapport *Onderzoek heterogeniteit asfaltbekledingen*. F. Arce, A.K. de Looff, KOAC-NPC, e0902633-2, augustus 2010.
- [9] Rapport *Golfklappen op asfalt, validatie van GOLFKLAP*, M. Klein Breteler, WL Delft, januari 2007, report H4134.
- [10] *WTI-2011: Voorschrift Toetsen op Veiligheid, Technisch Deel (VTV - Technisch deel); Concept Wettelijk Toetsinstrumentarium (WTI2011)*, Rijksoverheid 21 mei 2012.
- [11] Stowa publicatie *State of the art asfaltdijkbekledingen*, Stowa 2010, w06.
- [12] Paper *Shock pressure interactions on prototype sea dykes caused by breaking waves*. A. Führböter, U. Sparboom, in: Kolkman P.A. et al, (Eds) *Modelling Soil-Water-Structure Interactions (Sowas 88)*, Balkema, Rotterdam, 1988, p 243-252.
- [13] Rapport *Ontwikkeling restlevensduurmodel voor asfaltdijkbekledingen op basis van valgewichtdeflectiemetingen* (rapport e130108001), KOAC•NPC, 18 juli 2013
- [14] Memo *Wave attack on sea dikes - Sensitivity analysis*, by Alex Rohe Deltares 29<sup>th</sup> of May 2012, reference 1206016-001-GEO-0002.
- [15] Rapport *Gedrag van asfaltbekleding onder golfaanval*, WL Delft 1992, H1480
- [16] Rapport *Relatie tussen sterkte en stijfheid in de context van de inspectiemethode meerjarig onderzoek asfaltdijkbekledingen*, KOAC•NPC, 4 februari 2008, nummer e0700170-2.
- [17] Rapport *Vaststellen van verschillende invloeden op de Minersom ten behoeve van de modelfactor GOLFKLAP*, KOAC NPC 7 augustus 2014, nummer e140229701 (concept).
- [18] Rapport *Evaluatie interpretatie VGD-metingen naar aanleiding van de nieuwe procedure voor temperatuurcorrecties*; KOAC NPC 18 mei 2010, nummer e1000057-3.
- [19] Rapport *Evaluatie en analyse asfaltdijkbekledingen derde toetsronde*; KOAC NPC 6 juli 2012, nummer e120055001.
- [20] Report *Calibration of Safety Factors for wave impact on Hydraulic Asphalt Concrete Revetments*; WTI Cluster C, Deltares December 2014, report 1209431-010.
- [21] Report *Modelvergelijking golfklappen op een asfaltdijkbekleding*; KOAC NPC, July 2014; no. e140036801.
- [22] Report *Simulatie waterbouwasfaltbeton plaatmodel*; KOAC NPC January 2012; no. e110434401.

[23] Hydra-Ring 1.0; *Probabilistics toolbox for the WT12017; Validation document*. Version: 1.0 Revision: 3975; 29-11-2013.

[24] *Werkwijzebeschrijving voor het uitvoeren van een geavanceerde toetsing op golfklappen op een bekleding van open steenasfalt*. KOAC NPC 2014, rapport e130334101.